

The importance of model horizontal resolution on simulated precipitation in Europe – from global to regional models

Gustav Strandberg^{1,2}, Petter Lind^{1,2,3}

¹Rosby Centre, Swedish Meteorological and Hydrological Institute, SMHI, Norrköping, SE-602 19, Sweden

²Bolin Centre for climate research, Stockholm University, Stockholm, SE-106 91, Sweden

³Department of meteorology, Stockholm University, Stockholm, SE-106 19, Sweden

Correspondence to: Gustav Strandberg (gustav.strandberg@smhi.se)

Abstract. Precipitation is a key climate variable that affects large parts of society, especially in situations with excess amounts. Climate change projections show an intensified hydrological cycle through changes in intensity, frequency, and duration of precipitation events. Still, due to the complexity of precipitation processes and their large variability in time and space, climate models struggle to represent precipitation accurately. This study investigates the simulated precipitation in Europe in available climate model ensembles that cover a range of model horizontal resolutions. The ensembles used are: Global climate models (GCMs) from CMIP5 and CMIP6 (~100-300 km horizontal grid spacing at mid-latitudes), GCMs from the PRIMAVERA project at sparse (~80-160 km) and dense (~25-50 km) grid spacing and CORDEX regional climate models (RCMs) at sparse (~50 km) and dense (~12.5 km) grid spacing. The aim is to seasonally and regionally over Europe investigate the differences between models and model ensembles in the representation of the precipitation distribution in its entirety and through analysis of selected standard precipitation indices. In addition, the model ensemble performances are compared to gridded observations from E-OBS.

The impact of model resolution on simulated precipitation is evident. Overall, in all seasons and regions the largest differences between resolutions are seen for moderate and high precipitation rates, where the largest precipitation rates are seen in the RCMs with highest resolution (i.e. CORDEX 12.5 km) and smallest in the CMIP GCMs. However, when compared to E-OBS the high-resolution models most often overestimate high-intensity precipitation amounts, especially the CORDEX 12.5 km resolution models. An additional comparison to a regional data set of high-quality lends, on the other hand, more

28 confidence to the high-resolution model results. The effect of resolution is larger for precipitation
29 indices describing heavy precipitation (e.g. maximum one-day precipitation) than for indices describing
30 the large-scale atmospheric circulation (e.g. the number of precipitation days), especially in regions
31 with complex topography and in summer when precipitation is predominantly caused by convective
32 processes. Importantly, the systematic differences between low resolution and high resolution remain
33 also when all data are regridded to common grids of $0.5^{\circ} \times 0.5^{\circ}$ and $2^{\circ} \times 2^{\circ}$ prior to analysis. This shows
34 that the differences are effects of model physics and better resolved surface properties and not due to the
35 different grids on which the analysis is performed. PRIMAVERA high resolution and CORDEX low
36 resolution give similar results as they are of similar resolution.

37 Within the PRIMAVERA and CORDEX ensembles there are clear differences between the low- and
38 high-resolution simulations. Once reaching ~ 50 km the difference between different models is often
39 larger than between the low- and high-resolution versions of the same model. For indices describing
40 precipitation days and heavy precipitation the difference between two models can be twice as large as
41 the difference between two resolutions, in both the PRIMAVERA and CORDEX ensembles. Even
42 though increasing resolution improves the simulated precipitation in comparison to observations, the
43 inter-model variability is still large, particularly in summer when smaller scale processes and inter-
44 actions are more prevalent and model formulations (such as convective parameterizations) become
45 more important. .

46 **1 Introduction**

47 Precipitation is a key climate variable affecting the environment and human society in different ways
48 and on several temporal and spatial scales. In particular, heavy precipitation events may lead to large
49 damages caused by floods or landslides, while the absence of precipitation may cause droughts and has
50 impact on water- and hydropower supply. In recent decades there has therefore been extensive study,
51 and considerable advancement in our understanding, of the response of extreme precipitation to climate
52 change (O’Gorman, 2012; Kharin et al. 2013; Donat et al., 2016; Pfahl et al. 2017). For example, it is
53 widely held through theoretical considerations and model experiments that extremes will respond

54 differently than changes in mean precipitation (e.g. Allen and Ingram 2002; Pall et al 2007; Ban et al.,
55 2015).

56

57 Still, the simulation of precipitation in weather and climate models is challenging because of the wide
58 range of processes involved that acts and interacts on widely different temporal and spatial scales. An
59 accurate representation of precipitation in models requires skill in simulating (1) the large-scale
60 circulation, (2) interaction of the flow with the surface, and, (3) convection and cloud processes. With
61 the typical horizontal grid resolution of O (100 km) of global climate models (GCMs) point (1) can to a
62 large extent be properly represented but less so for (2) and (3) (e.g. van Haren et al., 2015; Champion et
63 al., 2011; Zappa et al., 2013). In particular, atmospheric convective processes are not resolved and
64 needs to be treated with convection parameterizations. As the range of scales resolved is broadened
65 through refining the horizontal grid spacing the simulation of precipitation generally improves. This is
66 achieved through more realistic representation of surface characteristics (such as topography, coastlines
67 and inland lakes and water bodies) and through more accurately solving the motion equations resulting
68 in more accurate horizontal moisture transport and moisture convergence (Giorgi and Marinucci 1996;
69 Gao et al. 2006; Prein et al. 2013a). Indeed, GCMs with ~25-50 km grid spacing show promise to
70 improve simulation of precipitation (van Haren et al., 2015; Delworth et al., 2012; Kinter et al., 2013;
71 Haarsma et al., 2016; Roberts et al., 2018a; Baker et al., 2019).

72

73 Dynamical down-scaling of GCMs with regional climate models (RCMs) allows for even finer grids
74 which leads to more detailed information of and further improvements in regional and local climate
75 features, for example spatial patterns and distributions of precipitation in areas of complex terrain
76 (Rauscher et al., 2010; Di Luca et al., 2011; Prein et al., 2013b). This can also have important
77 implications for climate change signals. Giorgi et al. (2016) found that an ensemble of RCMs at ~12 km
78 grid spacing showed consistently an increase in summer precipitation over the Alps region which
79 contrasted to the forcing GCMs that instead showed a decrease. The different responses were attributed
80 to increased convective rainfall in the RCMs due to enhanced potential instability by surface heating
81 and moistening at high altitudes not captured by the GCMs. Differences in the treatment of aerosols are

also identified as a reason for differences in climate response between RCMs and GCMs (Boé et al., 2020; Gutiérrez et al., 2020). RCMs are constrained by the lateral boundary conditions provided by the forcing GCM and studies of RCM ensembles have shown that the choice of forcing GCM have introduced the major part of the overall uncertainty in regional climate (e.g. Déqué et al., 2007; Kjellström et al., 2011). This effect is relatively more important for large-scale precipitation systems, for example frontal systems associated with extra-tropical cyclones. In seasons and regions when smaller scale processes like convection dominate, for example in summer over mid-latitudes, simulated precipitation is to a larger degree dependent of the RCM itself, in terms of grid resolution and sub-grid scale parameterizations (e.g. Iorio et al., 2004). A recent study investigated the effects of model resolution on local precipitation on short time scales and found that the 12.5 km simulations better represent daily and sub-daily extreme and mean precipitation, also when simulations are aggregated to 50 km (Prein et al., 2016). They note, however, that the results are highly dependent on which observations the simulations are compared with, and that improvements are seen for the ensemble mean, and not necessarily for each individual model. In similar studies as the present one Iles et al. (2019) and Demory et al. (2020) compare simulations from the CORDEX, CMIP5 and PRIMAVERA ensembles. The results show increases in precipitation with resolution and, when compared to a mixture of E-OBS and high spatial-resolution gridded national datasets, CMIP5 underestimates precipitation amounts while CORDEX overestimates it, the effect of grid resolution being largest in areas with complex topography. They also find that PRIMAVERA performs similarly to CORDEX when run on the same resolution, which is interesting regarding that the PRIMAVERA models are developed for low resolutions. Iles et al. (2019) concluded from the considerable inter-model differences that improvements are seen for the ensemble mean rather than for individual models.

Although increased grid resolution often leads to improved simulation of precipitation, convection is usually not resolved by the model dynamics, even at grid spacings of around 10 km, but is instead parameterized (although it might be possible to turn off the parameterization already at this kind of resolution (Vergara-Temprado et al., 2019)). The choice of convection parameterization can have various effects on the occurrence and amount as well as on the onset timing and location (e.g. Dai et al.,

1999; Dai 2006; Stratton and Stirling, 2012; Gao et al., 2017). Commonly, models with parameterized convection exhibit biases in the diurnal precipitation cycle (Liang, 2004; Brockhaus et al., 2008; Gao et al. 2017), sometimes regardless of increases in grid resolution (Dirmeyer et al., 2012). In addition, models of coarse resolution often suffer from simulating precipitation over too large area compared to observations, and usually also too many days with weak precipitation (the “drizzle” problem) (e.g. Dai, 2006, Stephens et al., 2010). At sufficiently high resolution (< 4 km) models start to largely resolve deep convection enabling the parameterization to be turned off, so called “convection-permitting” models (Prein et al., 2015; Vergada-Temprado et al., 2019). Convection-permitting regional climate models (CPRCMs) are widely shown to reduce, at least to some extent, these biases, most evidently by improving the match of the diurnal cycle to observations (e.g. Prein et al., 2013a; Ban et al., 2014; Brisson et al., 2016; Gao et al., 2017; Leutwyler et al., 2017; Belušić et al. 2020) and better representation of sub-daily high-intensity precipitation events (e.g. Ban et al., 2014; Kendon et al., 2014; Fosser et al., 2015; Lind et al., 2020) than models with parameterized convection. A major drawback using these high-resolution climate models is the very high computational cost, making their use in ensembles to only recently emerge (Coppola et al., 2018).

The aim of this study is to:

- i. Investigate to what extent a large number of global and regional climate models can reproduce observed daily precipitation climatologies and characteristics over Europe.
- ii. Investigate how model horizontal grid resolution in either global or regional models affect the simulated precipitation in Europe; are there systematic differences and if so, are these persistent for different parts of Europe and for different seasons.

To this end, GCMs of standard resolution from the CMIP5 (Climate Model Intercomparison Project phase 5, Taylor et al., 2012) are compared with GCMs which participated in the HighResMIP (High Resolution Model Intercomparison Project, Haarsma et al., 2016) experiment within the H2020-EU-project PRIMAVERA. These models are: ECMWF-IFS (Roberts et al., 2018b), HadGEM3-GC31 (Roberts et al., 2019), MPI-ESM1.2 (Gutjahr et al., 2019), CNRM-CM6.1 (Voldoire et al., 2019) and

EC-Earth3P (Haarsma et al., 2020). Furthermore, the first results from the CMIP6 (Climate Model Intercomparison Project phase 6, Eyring et al., 2016) GCMs are included in the analysis. The GCMs are compared with RCMs from CORDEX (COordinated Regional Downscaling EXperiment, Gutowski et al., 2016). This allows for comparisons of different generations of models, global versus regional models and the impact of model horizontal grid resolutions. For a few cases, the same model version has been applied at two different grid resolutions which allows for investigating the impact of resolution alone. The simulated daily precipitation is analysed both in terms of precipitation intensity distributions and through a collection of standard precipitation-based indices.

2 Models and Methods

2.1 Global and regional models

The models used in this study are a selection of CMIP5 global models (corresponding to ~100-300 km horizontal grid spacing at mid-latitudes); the high (~25-50 km) and low (~80-160 km) resolution versions of the PRIMAVERA global models and the first available runs from CMIP6 (~100-300 km); and finally, a selection of CORDEX RCMs (at 12.5 and 50 km mid-latitude grid spacing). The low-resolution versions in each model ensemble is called LR, and the high-resolution HR. Note that not the full CMIP5, CMIP6 and CORDEX ensembles are used, but rather “ensembles of opportunity” for which daily precipitation were readily available. Table 1 lists the GCM ensembles used. Table 2 lists the GCM RCM combinations used in the CORDEX ensembles. The simulated precipitation for all models is analysed over the PRUDENCE regions in Europe (Fig. 1; Christensen & Christensen, 2007). Prior to analysis all grid points over sea are filtered out, and then for each region and model we calculate precipitation characteristics for all remaining land grid points. The simulations are analysed on their native grids, because this is the kind of data that users of climate simulations will face, and since all interpolation may alter precipitation characteristics (Klingaman et al., 2017). Nevertheless, to investigate all aspects of changed resolution it is sometime necessary to compare simulations on a common grid. In these cases, the results are also aggregated to two common grids with $2^{\circ} \times 2^{\circ}$ and $0.5^{\circ} \times 0.5^{\circ}$ grid spacing respectively.

164

165 **2.2 Observations**

166 Climate model evaluation exercises often rely, when possible, on gridded reference data sets. In this
167 study daily precipitation sums in models are compared with data from E-OBS version 19.0e at 0.1° and
168 0.25° grid spacing (Cornes et al., 2018). E-OBS comprise daily station values interpolated onto a grid
169 that spans the entire European continent. The main advantage of using E-OBS is the large geographical
170 coverage at a relatively high resolution available over an extended (climatological) time period. It
171 enables a consistent model-observation comparison over the whole continental part of Europe, with its
172 varying climatological and environmental characteristics.

173 Gridded products, such as E-OBS, involves spatial analysis and interpolation of point measurements
174 onto a regular grid, and are inherently associated with uncertainties originating from both non-climatic
175 influences (e.g. inaccuracies in measurement devices or relocation of measurement sites) and from
176 sampling issues associated with weather and environmental conditions, for example in situations with
177 snowfall in windy conditions (Kotlarski et al. 2019; Rasmussen et al., 2012). The quality of such data
178 sets largely depends on the availability of stations to base the interpolation on, implying that in regions
179 where station density is low the quality of the gridded product is also lower (Herrera et al. 2019). For
180 precipitation this is of even greater importance due to its highly heterogeneous character in both time
181 and space, in particular for high-intensity precipitation events (extremes). These are often local in
182 character (temporally and spatially), even in cases when embedded in larger (synoptic) scale
183 precipitation systems, and can thus be heavily undersampled (Herrera et al. 2019; Prein and Gobiet
184 2017). Furthermore, mountainous areas act as strong forcing of precipitation giving rise to large spatial
185 variability over the terrain. Combined with the lack of dense networks of stations in these regions, and
186 usually also a higher occurrence of snowfall, makes it very difficult to achieve highly reliable data over
187 mountains (e.g. Hughes et al. 2017; Lundquist et al. 2019).

188 The quality of E-OBS varies over Europe (see Fig. 1 in Cornes et al. 2018); the station density is for
189 example very high over Scandinavia, Germany and Poland, while it is lower in Eastern Europe and in
190 the Mediterranean region. Gridded regional or national data sets may offer higher quality as these are

generally based on a denser station network and are often also provided with higher spatial and/or temporal resolution compared to E-OBS (Kotlarski et al. 2019, Prein and Gobiet 2017). Here, we limit the comparison to E-OBS only. However, to assess the impact of high-quality regional data, an additional analysis of the precipitation distributions was performed, using ASoP analysis (see Sec. 2.3), comparing models and E-OBS against the NGCD (Nordic Gridded Climate Dataset, Lussana et al. 2018) data set. NGCD is based on daily station data for precipitation and temperature, interpolated onto a 1x1 km grid covering Scandinavia.

2.3 ASoP and precipitation indices

To investigate the effect of model grid resolution on the full distributions of daily precipitation intensities, we use the ASoP (Analysing Scales of Precipitation) method (Klingaman et al., 2017; Berthou et al., 2018). ASoP involves splitting precipitation distributions into bins of different intensities and then provides information of the contributions from each precipitation intensity separately to the total mean precipitation rate (i.e. given by all intensities taken together). In the first step, precipitation intensities are binned in such a way that each bin contains a similar number of events, with the exception of the most intense events, which are rare. The actual contribution (in mm) of each bin to the total mean precipitation rate is obtained by multiplying the frequency of events by the mean precipitation rate. The sum of the actual contributions from all bins gives the total mean precipitation rate. The fractional contribution (in %) of each bin is further obtained by dividing the actual contributions by the mean precipitation rate. In this case, the sum of all fractional contributions is equal to one, thus the information provided by fractional contributions is predominantly about the shape of the distribution. Taking the absolute differences between two fractional distributions and sum over all bins gives a measure of the difference in the shapes of the precipitation distributions. This is here called the “Index of fractional contributions”. Since E-OBS precipitation intensities, in contrast to model data, are not continuous, the resulting ASoP factors for E-OBS tend to be noisy, especially for lower intensities. In order to facilitate the interpretation of the results, the regionally averaged ASoP factors for E-OBS were smoothed to some extent by using a simple filter.

219 The ASoP method is here applied to grid points pooled over target regions (Fig. 1) separately and the
220 result is a distribution for each model showing the probability of different precipitation intensities based
221 on daily precipitation. Most results presented here concern the actual contributions, both to limit the
222 number of figures and because these factors conveniently provide information on both shape of
223 distributions as well as the mean values. The ASoP distributions of all analysed models are used to
224 compare model behaviour and performance. In particular to see how changing the grid resolution affects
225 different parts of the distribution, for example if contributions from low and high precipitation
226 intensities are different.

227

228 In addition to ASoP, a number of indices based on daily precipitation (listed in Table 3) are calculated
229 for the same regions. For each model, the indices are calculated separately for each grid point within a
230 region (land points only), and the values are then pooled to calculate percentiles representing the region.
231 This also means that the calculated model spread reflects geographical and not temporal variability.
232 The index percentiles are represented by box plots (Sect. 3).

233 **3 Results**

234 **3.1 ASoP analysis**

235 **3.1.1 Annual precipitation**

236 Since the ASoP results are very similar between CMIP5 and CMIP6 GCMs (not shown), the results
237 presented here include only one of these ensembles, CMIP6. Figure 2 presents the actual contributions
238 (normalized bin frequency \times mean bin rate) for annual daily precipitation over four of the PRUDENCE
239 regions: Scandinavia, mid-Europe, the Alps and the Mediterranean. In general, the model ensembles
240 have higher amounts of precipitation compared to E-OBS, signified by larger contributions at low (< 2 -
241 3 mm day^{-1}) and moderate-to-high (> 5 - 10 mm day^{-1}) intensities. An exception is the CMIP6 ensemble
242 that instead shows lower contributions for moderate-to-high precipitation intensities, i.e. above 10 - 20
243 mm day^{-1} (Scandinavia, mid-Europe and the Alps) or between 5 - 20 mm day^{-1} (Mediterranean). CMIP6
244 also tends to have the largest overestimates of contributions from the lower intensities (below 5 mm

245 day⁻¹). Another consistent feature is that the probabilities for the higher intensities (above 15 mm day⁻¹)
 246 increase with increasing grid resolutions of respective model ensemble, and consequently the
 247 contributions become increasingly larger than E-OBS (Fig. 2). This is most evident for the Alps region
 248 where the CMIP6 models (100-300 km grid spacing) clearly give smaller contributions than E-OBS and
 249 the PRIMAVERA models (25-160 km), the latter having smaller contributions than the CORDEX LR
 250 models (50 km) and the CORDEX HR models (12.5 km). The higher resolution models peak at higher
 251 intensities and have wider distributions with larger contributions from high-intensity daily rates. The
 252 sensitivity of model grid resolution to precipitation amounts and variability in association with areas
 253 with complex and steep topography (e.g. Prein et al., 2015) is most likely the main reason for the large
 254 differences between model ensembles in the Alps region. For example, the upper end of the CMIP6
 255 distributions is around 50 mm day⁻¹ while corresponding part in CORDEX HR models is around 100
 256 mm day⁻¹ (bottom right panel in Fig. 2). To further verify the results, the same analysis was performed
 257 after all data had been interpolated (conservatively) to two common grids; one at 2°×2° resolution and
 258 one at 0.5°×0.5° degree resolution (Figs. S1 and S2 in Supplementary). The interpolation to either grid
 259 has an overall small impact on the results. With the coarser grid (2°×2°) the ASoP actual contributions
 260 have relatively larger contributions from the bulk part and a smaller contribution from the highest
 261 intensities, as expected from the smoothing effect of interpolation. These results provide increased
 262 confidence in the conclusions drawn from analysis on native grids.

263 **3.1.2 Seasonal precipitation**

264 Further insight can be gained by investigating seasonal differences (Fig. 3). In winter (DJF) the model
 265 ensemble means generally overestimate total mean precipitation compared to E-OBS (i.e. total areas
 266 under the curves showing differences are positive). The bulk of the distributions are slightly shifted to
 267 higher precipitation rates and also to higher contributions (except for the Mediterranean region). The
 268 largest inter-ensemble differences are seen for the Mediterranean where CORDEX HR shows the
 269 largest shift from E-OBS towards contributions from higher precipitation rates, and PRIMAVERA is
 270 similar to CORDEX LR. In summer (JJA), the ensemble means show larger contributions from
 271 intensities above 10-15 mm/day than E-OBS, especially in CORDEX HR. However, as this is in many

272 cases compensated by lower contributions from rates between 2-10, the total mean precipitation biases
273 are smaller than in winter. While the CORDEX ensemble means indicate larger total mean precipitation
274 in France and Mediterranean, CMIP6 produces in all regions higher contributions from low-to-moderate
275 ($< \sim 5$ mm/day) compared to E-OBS and lower contributions from higher intensities. Furthermore, there
276 is a tendency in all regions of a larger spread within each model ensemble in JJA than in DJF (see
277 coloured shadings in Fig. 3). Even though it is a very crude estimate of the spreads (the 5-95 percentile
278 range in respective model ensemble), it can be argued that the differences in part is related to the
279 seasonally prevailing weather conditions. In winter the North Atlantic storm track is in its active phase
280 with frequent passings of synoptic weather systems over Europe. These features are generally well
281 represented in climate models – hence larger consistency with associated precipitation across models. In
282 summer, on the other hand, synoptic activity is reduced and convective processes (either as isolated or
283 organized systems or embedded in larger scale features like fronts) become more prominent in
284 precipitation events. Sensitivity to model grid resolution and physics parameterizations (e.g. convection
285 parameterization) is larger during this season. The larger summertime spread in ensembles seen in Fig.
286 3 might then reflect larger uncertainties associated with model resolution and formulation. It is further
287 noted that the ensemble spread is not increased as much (from winter to summer) over northern/north-
288 western Europe which is relatively more affected by synoptic scale events during summer compared to
289 southern parts of Europe (not shown).

290

291 Model ensemble differences for all regions and seasons are summarized in Figure 4, with E-OBS as
292 reference. In spring (MAM) and winter (DJF) all ensembles have higher total mean precipitation in all
293 regions. In summer (JJA) and autumn (SON) biases are also mostly on the positive side but smaller
294 (primarily for GCM ensembles), and in some regions close to zero or slightly negative (e.g. the Alps,
295 East Europe, Iberian Peninsula). Often there is an indication of a positive correlation between
296 differences in mean (x-axis in Fig. 4) and differences in fractional contributions (y-axis, which indicates
297 overall differences in the shape of the distributions), as seen for example in France or Mid-Europe
298 regions. However, there are also cases with large differences in the shape but small total mean
299 precipitation biases, for example the CMIP ensembles in JJA and SON over the Alps, suggesting

compensating effects from different parts of the precipitation distribution. The overall spread is also highly variable between the regions; Scandinavia, Mid- and East-Europe and the British Isles are characterized by relatively smaller inter-ensemble differences, while in the Alps and Mediterranean the spread is large. The spread is in some regions dominated by inter-seasonal differences, e.g. in Mid-Europe and France, where typically the largest differences (in terms of both total means and distribution shapes) occur in DJF and MAM and smaller spreads in JJA and SON. In the Alps, Iberian Peninsula and the Mediterranean regions, however, the relatively larger inter-ensemble differences lead to an increased overall spread. Here, CORDEX HR further exhibits the largest differences to the GCM ensembles and also often larger deviations from E-OBS. These latter regions are either characterized by complex and steep topography (e.g. the Alps and the Pyrenees), large fraction of coastal areas and/or by relatively dry environments dominated by precipitation of convective nature (particularly for the warmer months). These factors most likely play important roles for the larger differences seen between the low resolution CMIP GCMs and the higher resolution PRIMAVERA GCMs and CORDEX RCMs, as well as contributing to larger uncertainties in, and lower quality and representativeness of, observational data. In contrast, in almost all seasons over the British Isles, the CORDEX HR biases in total precipitation compared to E-OBS are among the smallest with respect to the other ensembles (the difference in the shape is similar). Finally, it is noted that for all regions PRIMAVERA HR and CORDEX LR give comparable distributions as they are of similar resolution.

To summarize, we can conclude that, in comparison to E-OBS, most model ensembles exhibit larger contributions for most precipitation intensities, but most consistent for low ($< \text{ca } 3 \text{ mm day}^{-1}$) and moderate-to-high ($> \text{ca } 10 \text{ mm day}^{-1}$). The larger contributions occur predominantly in DJF while in summer there are often lower contributions than in E-OBS for moderate intensities (leading to smaller biases in total means). In general, the CORDEX ensembles, and most often also PRIMAVERA, show a shift towards larger contributions from higher intensities compared to CMIP ensembles, especially in areas with complex orography as in the Alps. The higher model grid resolution does not always lead to improvements, i.e. closer agreements to E-OBS. However, it is worth re-emphasizing that the quality of E-OBS observations can be significantly lower in certain regions (e.g. mountainous areas or areas with

low density of precipitation gauges) and seasons (especially in wintertime when the fraction of snowfall is largest which is more sensitive to wind induced undercatch) (Prein and Gobiet, 2017; Herrera et al., 2019), thus complicating the assessment of model behaviour in comparison to observations. To further highlight this issue, we have included an ASoP analysis for the Scandinavia region (Fig. S3) including a regional high-quality high-resolution gridded observational data set; NGCD (Lussana et al., 2018). In both DJF and JJA, the model ensembles still overestimate contributions from the bulk of the intensity distribution; however, NGCD has higher contributions from low intensities compared to E-OBS, reducing the model ensemble bias. More interestingly, NGCD shifts towards larger contributions for high intensities, $> 10 \text{ mm day}^{-1}$, in effect lending more credibility to the CORDEX HR ensemble and less to the others.

3.1.3 Effect of grid resolutions – a one-to-one comparison

For multi-model ensembles, the sensitivity to model grid resolutions can generally only be assessed qualitatively since other aspects, such as differences in model formulation, also contribute to differences in model performance. In other words, it cannot be definitely stated to what extent differences in performance comes from higher resolution or from other differences in the model code. For the PRIMAVERA models, however, it is possible to directly compare low- and high-resolution model versions. In CORDEX ensembles this is also possible to some extent for a few models where low- and high-resolution versions of RCMs have been forced by the same parent GCMs. This is the case for nine RCM-GCM combinations (6 different RCMs driven by 4 different GCMs). Note that, in contrast to PRIMAVERA, CORDEX LR-HR “pairs” may not use the same version of the common model, which could also influence the results in addition to change in grid resolution. Further, the magnitude of the grid resolution change (the *delta* value) is the same for CORDEX models ($\text{delta}=4$), while for PRIMAVERA models it varies between approximately 2 and 5. Figure 5 shows the one-to-one comparison for DJF and JJA for selected regions. For CORDEX models the high-resolution model versions generally generate, in both seasons, larger contributions from precipitation intensities above ca 10 mm day^{-1} . This is sometimes accompanied by lower contributions from lower rates as seen for example in Scandinavia and the Alps in DJF. Similar results are seen for PRIMAVERA although not as

consistently; e.g. over the British Isles and the Alps in JJA about half the models show increased contributions in the HR models over the bulk part, the other half showing instead lower contributions (although for higher rates most HR models show larger contributions). In fact, for many regions there is a larger spread in JJA within each model ensemble and also between the individual LR versus HR responses compared to DJF. It could be argued that this effect is related to precipitation events being of more convective nature in summer and thus larger sensitivity to model grid resolution as well as model physics. In winter, CORDEX RCMs are to a larger extent being influenced by the forcing GCMs and therefore, as there is only four different GCMs used in the nine RCM-GCM combinations shown here, tends to exhibit more similar responses in this season.

3.2 Selected precipitation-based indices

3.2.1 Model ensemble comparison

Figure 6 shows the number of precipitation days (RR1, Table 3) as simulated by all models for each PRUDENCE region. The number of precipitation days does not differ much between the model ensembles. There are clear differences between individual models, but it is difficult to establish any significant differences between the model ensembles. This is the case both for regions with a higher occurrence of precipitation days (e.g. SC) and regions with fewer precipitation days (e.g. IP). All models show about the same number of precipitation events over the whole year, which may suggest that the large-scale weather patterns are not influenced that much by higher resolution; also, when looking at individual seasons the differences between ensembles are small (Fig. S4). Note, however, that the large-scale circulation in the RCMs to a large extent is governed by the driving GCM which have typical resolutions of around 200 km. Interpolating the data to a common grid prior to analysis does not have a large impact on RR1 (Fig. S5). Most models overestimate the number of precipitation days compared to observations. It is a well-known feature of climate models, particularly those with parameterized convection, that they tend to have too many wet days (e.g. Dai, 2006; Stephens et al., 2010).

381 The number of days with large precipitation amounts, above 10 mm day⁻¹ and 20 mm day⁻¹, become
382 more frequent with higher model resolution. For example, the number of days with precipitation over 20
383 mm (R20mm, Table 3) increases from just a few in CMIP5 to 5-10, or even more, in CORDEX HR
384 (Fig. 7). The 10th to 90th inter-percentile range increases, due to a larger increase in the 90th percentile.
385 Generally, the spread is larger for models with high resolution. This could partly be explained by higher
386 number of data points in the high-resolution models (i.e. larger number of grid points); a high-resolution
387 model is more likely to better represent the spatial variations of precipitation within a region while in
388 coarser scale models precipitation fields are smoother due to fewer grid points. The differences between
389 resolutions remain, however, also when all data are interpolated to two common grids of 0.5°×0.5° and
390 2°×2° resolutions; the median and spread also remain similar in all ensembles. In small regions such as
391 AL the coarsest grid gives to few points, which means that it's difficult to calculate the 10th and 90th
392 percentiles. The spread in CORDEX HR increases when interpolated to 2°×2° because the points with
393 high values are not balanced by as many points close to the median (a 0.5°×0.5° grid contains 16 times
394 more points than a 2°×2° grid). Compared to E-OBS the average number of days with more than 20 mm
395 day⁻¹ is more accurately simulated in the high-resolution ensembles, but the spread is highly
396 exaggerated. The PRIMAVERA models have median values similar to E-OBS and also a more similar
397 spread. The signal is the same for the individual seasons, but less pronounced since the potential
398 number of days is smaller when divided over four seasons instead of counted over the whole year (Fig
399 S6). The effect of resolution is therefore clearest in the season where most days occur, which means
400 winter in western Europe and summer in central Europe.

401

402 The fact that the number of wet days is similar between LR and HR models (Fig. 6) but with increased
403 frequency of (heavy) precipitation in HR models (Fig. 7) suggests that, for the latter, the precipitation
404 intensity on the wet days is higher. This is shown in the simple precipitation intensity index (SDII,
405 Table 3, Fig. 8). SDII is indeed affected by resolution, at least between CMIP5/6 and CORDEX; the wet
406 day average precipitation is larger in the HR simulations compared to LR models, and also the intra-
407 model spread (spread between models within the ensemble) is larger. For all regions, SDII is higher in
408 the HR models. Perhaps, the relative increase in SDII is higher in regions with large spatial variations

(for example because of complex orography or coastlines) such as IP and AL. The median SDII values in high-resolution models are in all regions closer to E-OBS than the low-resolution models, even though the model spread is generally larger in the climate models than in E-OBS. The differences between ensembles remain both for the median and the spread when the data are regridded to common grids. Also, for individual seasons it is clear that SDII increases with higher resolution, but the SDII values do not vary much with season (Fig. S7).

The higher intensities for extreme precipitation in high-resolution models compared to low-resolution models are also seen in the maximum one-day (Rx1day, Table 3, Fig. 9) and maximum five-day precipitation (not shown). There is a clear increase in both intensities and intra model spread in the high-resolution models. It can be discussed if this increase is an improvement since the CORDEX HR models give a maximum one-day precipitation that is significantly larger than E-OBS. On the other hand, it can be discussed if E-OBS is able to reliably represent these extremes (Hofstra et al., 2009; Prein and Gobiet, 2017). The medians and the spreads remain more or less the same also when regridded to common grids. In small regions such as AL the spread is reduced because the number of data points is small when regridded to a coarse grid. In regions with large spatial variations (e.g. between coast and mountain) such as IP the spread increases because high values are not balanced by as many points with values close to the median. In winter the effect of higher resolution is mainly seen in regions with complex topography, while in summer there is a clear signal in all regions (Fig 10). This reflects that higher resolution makes the largest difference in complex topography and for convective precipitation events.

3.2.2 One-to-one comparison

We let the mid-Europe region (ME) represent the whole domain, as the same conclusions can be made for all regions, only with small differences in the number of models that give significant differences. A one-to-one comparison is made of the selected indices for the models where there is both a low and a high grid resolution version (Fig. 11). The LR and HR versions are compared with a Welsh's t-test

435 (Welsh, 1947) at the 0.05 significance level to see if the simulated indices are significantly different.
 436 This corroborates the analysis above, and adds further detail by quantifying the differences.
 437
 438 Although the difference in the number of precipitation days (RR1, Fig. 11, top row) is significant for
 439 most models it is not clear how it is affected by resolution. The differences are small, mainly within ± 10
 440 days year⁻¹, in some cases negative and in some positive. The differences between models are larger
 441 than the differences between resolutions. It is clear, however, that all models overestimate the number
 442 of precipitation days compared to E-OBS. This is true also when the data is regridded to common grids,
 443 but three models and E-OBS get insignificant differences when regridded to $2^\circ \times 2^\circ$ instead of only one
 444 model at the native grids.
 445
 446 The number of days with precipitation more than 20 mm (R20mm, Fig. 11, second row) is significantly
 447 different between HR and LR for all models and E-OBS. For the CORDEX models R20mm is higher in
 448 most HR versions, while the difference is less clear in the PRIMAVERA models. All simulations with
 449 the RCA4 RCM, regardless of the driving GCM, clearly show higher R20mm in the HR version
 450 compared to the LR versions, which indicates that the difference in the index mainly is a result of the
 451 changed grid resolution in the RCM. The differences between LR and HR remain also when regridded
 452 to common grids which means that this is an effect of differences in model physics. CORDEX LR is
 453 close to E-OBS, while CORDEX HR generally overestimates R20mm.
 454
 455 The simple precipitation intensity index (SDII, Fig. 11, third row) is significantly different in one out of
 456 four PRIMAVERA models and four out of nine CORDEX models. Differences are small, tenths of mm
 457 day⁻¹, for most models. Most significant differences disappear when regridded to $0.5^\circ \times 0.5^\circ$ and all
 458 disappear when regridded to $2^\circ \times 2^\circ$ suggesting that the resolution does not affect SDII much in these
 459 model pairs. We still see a difference between CMIP GCMs and CORDEX RCMs (cf. Fig 8).
 460
 461 The maximum one-day precipitation (Rx1day, Fig. 11, bottom row) is significantly different in the HR
 462 version in all but one model (a PRIMAVERA model). The HR versions have higher precipitation values

and larger spread in all but two PRIMAVERA models and one CORDEX model. Especially the CORDEX HR models have a higher maximum one-day precipitation. This seems to be driven by the RCM rather than the driving GCM. As an example, three RCMs are forced with the MPI-ESM-LR GCM. When forced by this GCM the Rx1day in the CCLM4-8-17 RCM is lower in the HR version, while in REMO2009 and RCA4 HR RCMs Rx1day is higher. In RCA4 the difference is particularly large, regardless of the driving GCM. That the differences result from differences in model physics is supported by the fact that the differences remain also when the data is regridded to common grids.

The one-to-one comparison of selected indices shows that there are significant differences between the LR and HR models and that these are results of differences in model performance and not only the number of data points. It also shows that for some indices the largest difference occurs between CMIP5/6 and PRIMAVERA HR, rather than between PRIMAVERA and CORDEX. This means that some of the differences seen in Figures 6-10 are not as clear in figure 11. The comparison also shows that even though there are significant differences between LR and HR it is for some cases difficult to establish significant differences between two ensembles since the difference between two models are often larger than between the LR and HR version of the same model.

It should be noted that the CORDEX RCMs are not always run with the same model version in the LR and HR simulations. Model differences could thus explain some of the differences between LR and HR. Since we don't have LR and HR simulations with all model versions we can't quantify this effect, only acknowledge it. It should also be noted that the difference in horizontal grid spacing varies between models. For CORDEX RCMs the resolution *delta* (LR/HR) is always 4 (50 km/12.5 km), but for PRIMAVERA it varies between 2 and 5. The *delta* value is larger in CORDEX than in most PRIMAVERA models, which could potentially mean that the effect of resolution is overestimated for the CORDEX RCMs. Figure 12 shows how the absolute differences in RR1, R20mm, SDII and Rx1day between the LR and HR version of the PRIMAVERA and CORDEX models described above correlates to the *delta* value in the ME region. There is no clear relation between the *delta* value and the size of the difference. CORDEX models that all have the same *delta* value span from small to large differences.

491 The spread between PRIMAVERA models is also quite large. This again suggests that the response of a
492 model to increased resolution depends on the model itself and not only on the magnitude of the
493 resolution change.

494 **4 Discussion and conclusions**

495 This study investigates the importance of model resolution on the simulated precipitation in Europe.
496 The aim is to investigate the differences between models and model ensembles, but also to evaluate
497 their performance compared to gridded observations. In a similar study Demory et al. (2020) compare
498 PRIMAVERA models with CORDEX LR and CORDEX HR. They conclude that CORDEX
499 indisputably improves the data from the driving CMIP5 models, but that the differences between
500 CORDEX LR and PRIMAVERA are generally small. Both ensembles perform well, but tend to
501 overestimate precipitation in winter and spring. The largest differences between the ensembles are for
502 high precipitation intensities, in especially summer, where PRIMAVERA gives less heavy precipitation
503 which makes it agree more with observations than CORDEX. Iles et al. (2020) compare the effect of
504 resolution on extreme precipitation in Europe in CMIP5 GCMs and CORDEX RCMs. They conclude
505 that high resolution models systematically produce higher frequencies of high-intensity precipitation
506 events. Our interpretation of this, given the results in our study, is that in some cases also the
507 overestimation of precipitation compared to E-OBS increases with higher resolution. The findings in
508 this study support the conclusions from the above-mentioned studies, and add details based on a wider
509 range of model ensembles and precipitation metrics. The fact that we come to the same conclusions as
510 Iles et al. (2019) and Demory et al (2020) with slightly different methods give strength to these
511 conclusions.

512 The ASoP analysis in this study shows that all model ensembles have larger contributions from heavy
513 precipitation in winter compared to E-OBS, and that the higher values become most prominent for the
514 ensemble with the highest grid resolution, CORDEX HR. The biases compared to E-OBS are generally
515 smaller in summer. The PRIMAVERA ensemble is in good agreement with observations and has
516 smaller bias than CORDEX for many regions. CMIP5 and CMIP6 mostly underestimate contributions

517 from moderate-to-high precipitation intensities in summer while overestimating low-intensity events.
518 Overall, in the summer season, the spread is large between ensembles and between models within the
519 ensembles. This is indicative of large uncertainties which are most likely related to uncertainties in how
520 models are able to treat smaller scale precipitation events involving convection. With respect to E-OBS,
521 the ASoP results partly show that higher horizontal grid resolution does not necessarily mean better.
522 However, in coastal regions and regions with steep or complex topography there are uncertainties in
523 both models and observations. Particularly in winter observations suffer from undercatch when
524 precipitation falls as snow during windy conditions and in summer, smaller scale convective
525 precipitation may be smoothed considerably or missed completely by ground rain gauges (which E-
526 OBS is based on). E-OBS is not based on the full network of rain gauges in all countries, which could
527 also lead to undercatch. Therefore, it is not always obvious which model or ensemble of models is
528 closest to reality. When compared to NGDC, a regional data set of high-quality, the difference between
529 CORDEX HR and observations is reduced, which gives more confidence to the high-resolution model
530 results.

531

532 It is clear that the horizontal resolution of a model has a large effect on precipitation, mostly on the
533 heavier precipitation and in areas with complex and steep orography. The number of precipitation days
534 does not depend much on resolution as this is mostly depending on large scale weather patterns and not
535 so much on local topography and convection. For heavy precipitation events, which often are more local
536 and short-lived in character, model resolution is more important. The high-resolution models better
537 resolve such events and distinguish better between different parts of a region. Thus, extreme
538 precipitation is more intense and more frequent in the HR models compared to the LR models in this
539 study. With the same amount of wet days this means that precipitation intensifies so that the wet days
540 get wetter. The largest impact of increased model scale resolution on precipitation is most evident for
541 the coarser scale models; increasing the resolution from CMIP5/6 to PRIMAVERA HR has a greater
542 effect than increasing from CORDEX LR/PRIMAVERA HR to CORDEX HR. This does not, however,
543 mean that increased resolution gets less and less worthwhile; further refining the grid until convection-
544 permitting resolutions are reached (less than ~ 5 km grid spacing), in which case convection

parameterizations may be turned off, has a large positive effect (e.g. Prein et al. 2015). This is not shown here as the smallest grid spacing in models in this study is 12.5 km. The effect of higher resolution is seen in regions with small amounts of precipitation as well as regions with high amounts of precipitation, and in regions with small and large geographical differences. The higher percentiles change more than the low percentiles for all studied indices. Increasing resolution has about the same effect on both GCMs and RCMs, furthermore GCMs and RCMs of comparable resolution simulate comparable precipitation climates, even though PRIMAVERA is often drier than CORDEX.

It is worth to note that the differences between RCM simulations, and how they respond to differences in resolution, may very well be explained by the driving GCM and the state of the atmospheric general circulation in them (Kjellström et al., 2018; Sørland et al., 2018; Vautard et al., 2020). Higher resolution is expected to give a better described and more detailed climate, with for example deeper cyclones and more intense local showers; in a sense with more pronounced weather events. If two models are in different states, for example when it comes to where storm tracks cross Europe, and if these states are pronounced, that may lead to even larger model differences. Instead of a weak storm track in the south and a weak storm track in the north in the low-resolution model, we may now instead have strong storm tracks, which mean that the difference between the models increases. Still, the largest differences are seen in the CORDEX ensemble where the LR and HR models are run with the same coarse resolution GCM. This suggests that (regional) model resolution and performance is what determines high precipitation rates, rather than the driving GCM. To fully answer that would require an analysis of the circulation patterns in the different models. This is not done here, but should be a topic for further studies.

The differences between LR and HR largely remain also when the results are regridded to common grids of $0.5^{\circ} \times 0.5^{\circ}$ and $2^{\circ} \times 2^{\circ}$ which means that the HR version performs differently than the LR version of the same model, mainly because of better representations of topography and convection. The largest seasonal differences are seen for the heavy precipitation (R20mm, Rx1day). Heavy precipitation events

usually occur locally in summer which makes it more sensitive to model resolution. Difference in resolution has a larger impact on heavy precipitation in summer than in winter.

Higher resolution does not necessarily mean better results. If a model is already too wet the increase in heavy precipitation that is induced by the higher resolution means that the HR version agrees less with observations than the LR version. For the individual model it is possible to quantify the difference and improvement between LR and HR. On the ensemble level this is more difficult. The difference between different models is often larger than between LR and HR versions of the same model. In this sense the quality of an ensemble is depending more on the models it consists of rather than the average resolution of the ensemble. Furthermore, when downscaling with an RCM, the simulated extreme precipitation, and the differences between GCM and RCM, depends more on the used RCM and less on the downscaling itself, especially for heavy precipitation and particularly in summer.

Acknowledgements

The authors would like to thank Ségolène Berthou and two anonymous reviewers for giving valuable comments on the manuscript. This work has been funded by the PRIMAVERA project, which is funded by the European Union's Horizon 2020 programme, Grant Agreement no. 641727PRIMAVERA. This work used JASMIN, the UK collaborative data analysis facility. Some analyses were performed on the Swedish climate computing resource Bi provided by the Swedish National Infrastructure for Computing (SNIC) at the Swedish National Supercomputing Centre (NSC) at Linköping University. We acknowledge the E-OBS dataset from the EU-FP6 project UERRA (<http://www.uerra.eu>) and the Copernicus Climate Change Service, and the data providers in the ECA&D project (<https://www.ecad.eu>). We thank the modelling groups that run models and provide data within CMIP5, CMIP6, PRIMAVERA and CORDEX.

Data: The data are stored on the Jasmin infrastructure, <http://www.ceda.ac.uk/projects/jasmin/>. The simulations are part of the High Resolution Model Intercomparison project (HiResMIP) and will be

598 uploaded to the ESGF: <https://esgf-node.llnl.gov>. Scripts for analysing the data will be available from
599 the corresponding authors upon reasonable request.

600

601

602 **References**

603 Allen, M., and Ingram, W.: Constraints on future changes in climate and the hydrologic
604 cycle. *Nature* 419, 228–232 (2002). <https://doi.org/10.1038/nature01092>, 2002.

605

606 Baker, A. J., Schiemann, R., Hodges, K. I., Demory, M.-E., Mizielinski, M. S., Roberts, M. J.,
607 Schaffrey, L. C., Strachan, J. and Vidale P. L.: Enhanced Climate Change Response of Wintertime
608 North Atlantic Circulation, Cyclonic Activity, and Precipitation in a 25-km-Resolution, Global
609 Atmospheric Model. *J. Climate*, 32, 7763–7781, <https://doi.org/10.1175/JCLI-D-19-0054.1>, 2019.

610

611 Ban, N., Schmidli, J., and Schär, C.: Evaluation of the convection-resolving regional climate modeling
612 approach in decade-long simulations, *J. Geophys. Res. Atmos.*, 119: 7889– 7907,
613 doi:10.1002/2014JD021478, 2014.

614

615 Ban N., Schmidli, J., and Schär, C.: Heavy precipitation in a changing climate: Does short-term
616 summer precipitation increase faster?, *Geophys. Res. Lett.*, 42, 1165–1172,
617 <https://doi.org/10.1002/2014GL062588>, 2015.

618

619 Belušić, D., de Vries, H., Dobler, A., Landgren, O., Lind, P., Lindstedt, D., Pedersen, R. A., Sánchez-
620 Perrino, J. C., Toivonen, E., van Uft, B., Wang, F., Andrae, U., Batrak, Y., Kjellström, E., Lenderink,
621 G., Nikulin, G., Pietikäinen, J.-P., Rodríguez-Camino, E., Samuelsson, P., van Meijgaard, E. and Wu.,
622 M.: HCLIM38: a flexible regional climate model applicable for different climate zones from coarse to

623 convection-permitting scales, *Geosci. Model Dev.*, 13, 1311–1333, doi: 10.5194/gmd-13-1311-2020,
 624 2020.

625

626 Berthou, S., Kendon, E. J., Chan, S. C., Ban, N., Leutwyler, D., Schär, C. and Fosser, G.: Pan-European
 627 climate at convection-permitting scale: a model intercomparison study, *Clim. Dyn.*,
 628 doi:10.1007/s00382-018-4114-6, 2018.

629

630 Brisson, E., Van Weverberg, K., Demuzere, M., Devis, A., Saeed, S., Stengel, M., van Lipzig, N. P. M.:
 631 How well can a convection-permitting climate model reproduce decadal statistics of precipitation,
 632 temperature and cloud characteristics? *Clim. Dyn.*, 47: 3043–3061. doi:10.1007/s00382-016-3012-z,
 633 2016.

634

635 Brockhaus, P., Lüthi, D. and Schär, C.: Aspects of the diurnal cycle in a regional climate model, *Meteor.*
 636 *Z.*, 17: 433–443, doi:10.1127/0941-2948/2008/0316, 2008.

637

638 Boé, J., Somot, S., Corre, L., and Nabat, P.: Large differences in Summer climate change over
 639 Europe as projected by global and regional climate models: causes and consequences, *Clim. Dynam.*,
 640 54, 2981–3002, <https://doi.org/10.1007/s00382-020-05153-1>, 2020.

641

642 Champion, A. J., Hodges, K. I., Bengtsson, L. O., Keenlyside, N. S., and Esch, M.: Impact of increasing
 643 resolution and a warmer climate on extreme weather from Northern Hemisphere extratropical cyclones,
 644 *Tellus A: Dynamic Meteorology and Oceanography*, 63, 5, 893–906, DOI: 10.1111/j.1600-
 645 0870.2011.00538.x, 2011.

646

647 Christensen, J. H. and Christensen, O. B.: A summary of the PRUDENCE model projections of changes
 648 in European climate by the end of this century, *Climatic Change* 81, 7–30,
 649 <https://doi.org/10.1007/s10584-006-9210-7>, 2007.

650

651 Coppola, E., Sobolowski, S., Pichelli, E., Raffaele, F., Ahrens, B., Anders, I., Ban, N., Bastin, S., Belda,
 652 M., Belusic, D., Caldas-Alvarez, A., Cardoso, R. M., Davolio, S., Dobler, A., Fernandez, J., Fita, L.,
 653 Fumiere, Q., Giorgi, F., Görden, K., Güttler, I., Halenka, T., Heinzeller, D., Hodnebrog, Ø., Jacob, D.,
 654 Kartsios, S., Katragkou, E., Kendon, E., Khodayar, S., Kunstmann, H., Knist, S., Lavín-Gullón, A.,
 655 Lind, P., Lorenz, T., Maraun, D., Marelle, L., van Meijgaard, E., Milovac, J., Myhre, G., Panitz, H.-J.,
 656 Piazza, M., Raffa, M., Raub, T., Rockel, B., Scär, C., Sieck, K., Soares, M. M., Somot, S., Srnec, L.,
 657 Stocchi, P., Tölle, M. H., Truhetz, H., Vautard, R., de Vries, H. and Warrch-Sagi, K.: A first-of-its-kind
 658 multi-model convection permitting ensemble for investigating convective phenomena over Europe and
 659 the Mediterranean, *Clim. Dyn.* 55, 3–34, <https://doi.org/10.1007/s00382-018-4521-8>, 2018.
 660
 661 Cornes, R., van der Schrier, G., van den Besselaar, E. J. M., Jones, P. D.: An Ensemble Version of the
 662 E-OBS Temperature and Precipitation Datasets, *J. Geophys. Res. Atmos.*, 123.
 663 doi:10.1029/2017JD028200, 2018.
 664
 665 Dai, A.: Precipitation characteristics in eighteen coupled climate models, *J. Climate*, 19: 4605-4630,
 666 doi:10.1175/JCLI3884.1., 2006.
 667
 668 Dai, A., Trenberth, K. E.: The diurnal cycle and its depiction in the community climate system model, *J.*
 669 *Climate*, 17: 930-951, doi:10.1175/1520-0442, 2004.
 670
 671 Dai, A., Giorgi, F., and Trenberth, K. E.: Observed and model-simulated diurnal cycles of precipitation
 672 over the contiguous United States, *J. Geophys. Res.*, 104(D6), 6377– 6402, doi:10.1029/98JD02720,
 673 1999.
 674
 675 Delworth, T. L, Rosati, A., Anderson, W., Adcroft, A. J., Balaji, V., Benson, R., Dixon, K., Griffies,
 676 S.M., Lee, H. C., Pacanowski, R. C., Vecchi, G. A., Wittenberg, A. T., Zeng, F., and Zhang, R.:
 677 Simulated climate and climate change in the GFDL CM2.5 high-resolution coupledclimate
 678 model, *J. Clim.* 25, 2755–2781, doi:10.1175/JCLI-D-11-00316.1, 2015.

679

680 Demory, M.-E., Berthou, S., Sørland, S. L., Roberts, M. J., Beyerle, U., Seddon, J., Haarsma, R., Schär,
681 C., Christensen, O. B., Fealy, R., Fernandez, J., Nikulin, G., Peano, D., Putrasahan, D., Roberts, C. D.,
682 Steger, C., Teichmann, C., and Vautard, R.: Can high-resolution GCMs reach the level of information
683 provided by 12–50 km CORDEX RCMs in terms of daily precipitation distribution?, *Geosci. Model*
684 *Dev. Discuss.*, <https://doi.org/10.5194/gmd-2019-370>, in review, 2020.

685

686 Déqué, M., Rowell, D. P., Lüthi, D., Giorgi, F., Christensen, J. H., Rockel, B., Jacob, D., Kjellström, E.,
687 de Castro, M. and van den Hurk, B.: An intercomparison of regional climate simulations for Europe:
688 assessing uncertainties in model projections, *Climatic Change* 81, 53–70,
689 <https://doi.org/10.1007/s10584-006-9228-x>, 2007.

690

691 Dirmeyer, P. A., Cash, B. A., Kinter, J. L., Jung, T., Marx, L., Satoh, M., Stan, C., Tomita, H., Towers,
692 P., Wedi, N. and Achuthavarier, D.: Simulating the diurnal cycle of rainfall in global climate models:
693 Resolution versus parameterization. *Clim. Dyn.* 39(1–2):399–418, 2012.

694

695 Di Luca, A., de Elía, R. and Laprise, R.: Potential for added value in precipitation simulated by high-
696 resolution nested Regional Climate Models and observations, *Clim. Dyn.* 38, 1229–1247,
697 <https://doi.org/10.1007/s00382-011-1068-3>, 2011.

698

699 Donat, M., Lowry, A., Alexander, L., O’Gorman, P. A. and Maher, N.: More extreme precipitation in
700 the world’s dry and wet regions, *Nature Clim. Change* 6, 508–513,
701 <https://doi.org/10.1038/nclimate2941>, 2016.

702

703 Eyring, V., Bony, S., Meehl, G. A., Senior, C. A., Stevens, B., Stouffer, R. J., and Taylor, K. E.:
704 Overview of the Coupled Model Intercomparison Project Phase 6 (CMIP6) experimental design and
705 organization, *Geosci. Model Dev.*, 9, 1937–1958, doi:10.5194/gmd-9-1937-2016, 2016.

706

707 Fossler, G., Khodayar, S., Berg, P.: Benefit of convection permitting climate model simulations in the
 708 representation of convective precipitation, *Clim. Dyn.*, 44: 45-60, doi:10.1007/s00382-014-2242-1,
 709 2015.

710

711 Gao, X., Xu, Y., Zhao, Z., Pal, J. S. and Giorgi, F.: On the role of resolution and topography in the
 712 simulation of East Asia precipitation. *Theor. Appl. Climatol.* 86, 173–185:
 713 <https://doi.org/10.1007/s00704-005-0214-4>, 2006.

714

715 Gao, Y., Leung, L. R., Zhao, C., and Hagos, S.: Sensitivity of U.S. summer precipitation to model
 716 resolution and convective parameterizations across gray zone resolutions, *J. Geophys. Res. Atmos.*,
 717 122: 2714-2733, doi:10.1002/2016JD025896, 2017.

718

719 Giorgi, F., and Marinucci, M. R.: A Investigation of the Sensitivity of Simulated Precipitation to Model
 720 Resolution and Its Implications for Climate Studies, *Mon. Wea. Rev.*, 124, 148–
 721 166, [https://doi.org/10.1175/1520-0493\(1996\)](https://doi.org/10.1175/1520-0493(1996)), 1996

722

723 Giorgi, F., Torma, C., Coppola, E., Ban, N., Schär, C. and Somot, S.: Enhanced summer convective
 724 rainfall at Alpine high elevations in response to climate warming, *Nature Geosci.* 9, 584–589,
 725 <https://doi.org/10.1038/ngeo2761>, 2016.

726

727 Gutjahr, O., Putrasahan, D., Lohmann, K., Jungclaus, J. H., von Storch, J.-S., Brüggemann, N.,
 728 Haak, H., and Stössel, A.: Max Planck Institute Earth System Model(MPI-ESM1.2) for the
 729 High-Resolution Model Intercomparison Project (HighResMIP), *Geosci. Model Dev.*, 12, 3241–
 730 3281, <https://doi.org/10.5194/gmd-12-3241-2019>, 2019.

731

732 Gutiérrez, C., Somot, S., Nabat, P., Mallet, M., Corre, L., van Meijgaard, E., Perpiñán, O., and Gaertner,
 733 M. A.: Future evolution of surface solar radiation and photovoltaic potential in Europe: investigating
 734 the role of aerosols, *Environ. Res. Lett.*, 15, 034035, <https://doi.org/10.1088/1748-9326/ab6666>, 2020.

735

736 Gutowski Jr., W. J., Giorgi, F., Timbal, B., Frigon, A., Jacob, D., Kang, H.-S., Raghavan, K., Lee, B.,
737 Lennard, C., Nikulin, G., O'Rourke, E., Rixen, M., Solman, S., Stephenson, T., and Tangang, F.: WCRP
738 COordinated Regional Downscaling EXperiment (CORDEX): a diagnostic MIP for CMIP6, *Geosci.*
739 *Model Dev.*, 9, 4087-4095, doi:10.5194/gmd-9-4087-2016, 2016.

740

741 Haarsma, R. J., Roberts, M. J., Vidale, P. L., Senior, C. A., Bellucci, A., Bao, Q., Chang, P.,
742 Corti, S., Fučkar, N. S., Guemas, V., von Hardenberg, J., Hazeleger, W., Kodama, C., Koenigk,
743 T., Leung, L. R., Lu, J., Luo, J.-J., Mao, J., Mizielinski, M. S., Mizuta, R., Nobre, P., Satoh,
744 M., Scoccimarro, E., Semmler, T., Small, J., and von Storch, J.-S.: High Resolution Model
745 Intercomparison Project (HighResMIP v1.0) for CMIP6, *Geosci. Model Dev.*, 9, 4185–
746 4208, <https://doi.org/10.5194/gmd-9-4185-2016>, 2016.

747

748 Haarsma, R., Acosta, M., Bakhshi, R., Bretonnière, P.-A. B., Caron, L.-P., Castrillo, M., Corti, S.,
749 Davini, P., Exarchou, E., Fabiano, F., Fladrich, U., Fuentes Franco, R., García-Serrano, J., von
750 Hardenberg, J., Koenigk, T., Levine, X., Meccia, V., van Noije, T., van den Oord, G., Palmeiro, F.
751 M., Rodrigo, M., Ruprich-Robert, Y., Le Sager, P., Tourigny, É., Wang, S., van Weele, M., and
752 Wyser, K.: HighResMIP versions of EC-Earth: EC-Earth3P and EC-Earth3P-HR. Description,
753 model performance, data handling and validation, *Geosci. Model Dev. Discuss.*,
754 <https://doi.org/10.5194/gmd-2019-350>, in review, 2020.

755

756 Herrera, S, Kotlarski, S, Soares, PMM, et al. Uncertainty in gridded precipitation products: Influence of
757 station density, interpolation method and grid resolution. *Int J Climatol.* 2019; 39: 3717–
758 3729. <https://doi.org/10.1002/joc.5878>

759

760 Hofstra, N., Haylock, M., New, M. and Jones, P. D.: Testing E-OBS European high-resolution gridded
761 data set of daily precipitation and surface temperature, *J. Geophys. Res.*, 114, D21101,
762 doi:10.1029/2009JD011799, 2009.

763

764 Hughes, M., Lundquist, J.D. & Henn, B. Dynamical downscaling improves upon gridded precipitation
765 products in the Sierra Nevada, California. *Clim Dyn* 55, 111–129 (2020).
766 <https://doi.org/10.1007/s00382-017-3631-z>

767

768 Iles, C. E., Vautard, R., Strachan, J., Joussaume, S., Eggen, B. R., and Hewitt, C. D.: The benefits of
769 increasing resolution in global and regional climate simulations for European climate extremes,
770 *Geoscientific Model Development Discussion*, <https://doi.org/10.5194/gmd-2019-253>, 2019.

771

772 Iorio, J.P., Duffy, P.B., Govindasamy, B., Khairoutdinov, M., and Randall, D.: Thomson S. L., et al.:
773 Effects of model resolution and subgrid-scale physics on the simulation of precipitation in the
774 continental United States, *Climate Dynamics* 23, 243–258, <https://doi.org/10.1007/s00382-004-0440-y>,
775 2004.

776

777 Kendon, E. J., Roberts, N. M., Fowler, H. J., Roberts, M. J., Chan, S. C., Senior, C. A.: Heavier summer
778 downpours with climate change revealed by weather forecast resolution model, *Nat. Clim. Change* 4:
779 570–576, doi:10.1038/nclimate2258, 2014.

780

781 Kharin, V. V., Zwiers, F. W., Zhang, X. and Wehner, M.: Changes in temperature and precipitation
782 extremes in the CMIP5 ensemble, *Climatic Change* 119, 345–357 (2013).
783 <https://doi.org/10.1007/s10584-013-0705-8>, 2013.

784

785 Kinter III, J. L., Cash, B., Achuthavarier, D., Adams, J., Altshuler, E., Dirmeyer, P., Doty, B.,
786 Huang, B., Jin, E. K., Marx, L., Manganello, J., Stan, C., Wakefield, T., Palmer, T., Hamrud,
787 M., Jung, T., Miller, M., Towers, P., Wedi, N., Satoh, M., Tomita, H., Kodama, C., Nasuno,
788 T., Oouchi, K., Yamada, Y., Taniguchi, H., Andrews, P., Baer, T., Ezel, I. M., Halloy, C., John,
789 D., Loftis, B., Mohr, R., and Wong, K.: Revolutionizing climate modeling with project Athena: a multi-

790 institutional, international collaboration, Bull. Am. Meteorol. Soc., 94, 231–245, doi:10.1175/BAMS-
 791 D-11-00043.1, 2013.

792

793 Kjellström, E., Nikulin, G., Hansson, U., Strandberg, G. and Ullerstig, A.: 21st century changes in the
 794 European climate: uncertainties derived from an ensemble of regional climate model simulations, Tellus
 795 A: Dynamic Meteorology and Oceanography, 63:1, 24-40, DOI: 10.1111/j.1600-0870.2010.00475.x,
 796 2011.

797

798 Kjellström, E., Nikulin, G., Strandberg, G., Christensen, O. B., Jacob, D., Keuler, K., Lenderink, G.,
 799 van Meijgaard, E., Schär, C., Somot, S., Sørland, S. L., Teichmann, C., and Vautard, R.: European
 800 climate change at global mean temperature increases of 1.5 and 2 °C above pre-industrial conditions as
 801 simulated by the EURO-CORDEX regional climate models, Earth Syst. Dynam., 9, 459–478,
 802 <https://doi.org/10.5194/esd-9-459-2018>, 2018.

803

804 Klingaman, N. P., Martin, G. M., and Moise, A.: ASoP (v1.0): a set of methods for analyzing scales of
 805 precipitation in general circulation models, Geoscientific Model Development, 10(1), 57–83.
 806 <https://doi.org/10.5194/gmd-10-57-2017>, 2017.

807

808 Kotlarski, S., Szabó, P., Herrera, S., et al. Observational uncertainty and regional climate model
 809 evaluation: A pan-European perspective. Int J Climatol. 2019; 39: 3730–
 810 3749. <https://doi.org/10.1002/joc.5249>

811

812 Leutwyler, D., Lüthi, D., Ban, N., Fuhrer, O. and Schär, C.: Evaluation of the convection-resolving
 813 climate modeling approach on continental scales, J. Geophys. Res. Atmos., 122, 5237– 5258,
 814 doi:10.1002/2016JD026013, 2017.

815

816 Liang, X.-Z., Li, L., Dai, A., and Kunkel, K. E.: Regional climate model simulation of summer
817 precipitation diurnal cycle over the United States, *Geophys. Res. Lett.*, 31, L24208,
818 doi:10.1029/2004GL021054, 2004.

819

820 Lind, P., Belušić, D., Christensen, O. B., Dobler, A., Kjellström, E., Landgren, O., Lindstedt, D., Matte,
821 D., Pedersen, R. A., Toivonen, E., and Wang, F.: Benefits and added value of convection-permitting
822 climate modeling over Fenno-Scandinavia, *Climate Dynamics*, accepted, 2020.

823

824 Lundquist, J., M. Hughes, E. Gutmann, and S. Kapnick, 2019: Our Skill in Modeling Mountain Rain
825 and Snow is Bypassing the Skill of Our Observational Networks. *Bull. Amer. Meteor. Soc.*, 100, 2473–
826 2490, <https://doi.org/10.1175/BAMS-D-19-0001.1>.

827

828 Lussana, C., Saloranta, T., Skaugen, T., Magnusson, J., Tveito, O. E., and Andersen, J.: seNorge2 daily
829 precipitation, an observational gridded dataset over Norway from 1957 to the present day, *Earth Syst.*
830 *Sci. Data*, 10, 235–249, <https://doi.org/10.5194/essd-10-235-2018>, 2018

831

832 O’Gorman, P.: Sensitivity of tropical precipitation extremes to climate change, *Nature Geosci.* 5, 697–
833 700, <https://doi.org/10.1038/ngeo1568>, 2012.

834

835 Pall, P., Allen, M. R. and Stone, D. A.: Testing the Clausius–Clapeyron constraint on changes in
836 extreme precipitation under CO2 warming. *Clim. Dyn.* 28, 351–363, [https://doi.org/10.1007/s00382-](https://doi.org/10.1007/s00382-006-0180-2)
837 [006-0180-2](https://doi.org/10.1007/s00382-006-0180-2), 2007.

838

839 Pfahl, S., O’Gorman, P. and Fischer, E.: Understanding the regional pattern of projected future changes
840 in extreme precipitation. *Nature Clim. Change* 7, 423–427, <https://doi.org/10.1038/nclimate3287>, 2017.

841

842 Prein, A. F. and Gobiet, A.: Impacts of uncertainties in European gridded precipitation observations on
843 regional climate analysis, *Int. J. Climatol.*, 37, 305–327, doi:10.1002/joc.4706, 2017

844

845 Prein, A. F., Gobiet, A., Suklitsch, M., Truhetz, H., Awan, N. K., Keuler, K. and Georgievski, G.:
846 Added value of convection permitting seasonal simulations. *Clim. Dyn.*, 41 (9-10): 2655-2677.
847 doi:10.1007/s00382-013-1744-6, 2013a.

848

849 Prein, A. F., Holland, G. J., Rasmussen, R. M., Done, J., Ikeda, K., Clark, M. P. and Liu, C. H.:
850 Importance of Regional Climate Model Grid Spacing for the Simulation of Heavy Precipitation in the
851 Colorado Headwaters. *J. Climate*, 26: 4848–4857, doi: 10.1175/JCLI-D-12-00727.1, 2013b.

852

853 Prein, A. F., Langhans, W., Fosser, G., Ferrone, A., Ban, N., Goergen, K., Keller, M., Tölle, M.,
854 Gutjahr, O., Feser, F., Brisson, E., Kollet, S., Schidli, J., van Lipzig, N. P. M. and Leung, R.: A review
855 on regional convection-permitting climate modeling: Demonstrations, prospects, and challenges, *Rev.*
856 *Geophys.*, 53: 323– 361. doi:10.1002/2014RG000475, 2015.

857

858 Prein, A.F., Gobiet, A., Truhetz, H. et al. Precipitation in the EURO-CORDEX 0.11°0.11° and
859 0.44°0.44° simulations: high resolution, high benefits?. *Clim Dyn* 46, 383–412 (2016).
860 <https://doi.org/10.1007/s00382-015-2589-y>

861

862 Rasmussen, R., Baker, B., Kochendorfer, J., Myers, T., Landolt, S., Fischer, A., Black, J., Thériault, J.,
863 Kucera, P., Gochis, D., Smith, C., Nitu, R., Hall, M., Cristanelli, S. and Gutmann, A.: How well are we
864 measuring snow: the NOAA/FAA/NCAR winter precipitation test bed. *Bull. Am. Met. Soc.*, 93.
865 doi:10.1175/BAMS-D-11-00052.1, 2012.

866

867 Rauscher, S.A., Coppola, E., Piani and Giorgi F.: Resolution effects on regional climate model
868 simulations of seasonal precipitation over Europe. *Clim. Dyn.* 35, 685–711,
869 <https://doi.org/10.1007/s00382-009-0607-7>, 2010.

870

871 Roberts, M. J., Vidale, P. L., Senior, C., Hewitt, H. T., Bates, C., Berthou, S., Chang, P., Christensen, H.
872 M., Danilov, S., Demory, M.-E., Griffies, S. M., Haarsma, R., Jung, T., Martin, G., Minobe, S.,
873 Ringler, T., Satoh, M., Schiemann, R., Scoccimarro, E., Stephens, G., and Wehner, M. F.: The
874 Benefits of Global High Resolution for Climate Simulation: Process Understanding and the Enabling of
875 Stakeholder Decisions at the Regional Scale, *B. Am. Meteorol. Soc.*, 99, 2341–2359,
876 <https://doi.org/10.1175/BAMS-D-15-00320.1>, 2018a.

877

878 Roberts, C. D., Senan, R., Molteni, F., Boussetta, S., Mayer, M., and Keeley, S. P. E.: Climate model
879 configurations of the ECMWF Integrated Forecasting System (ECMWF-IFS cycle 43r1) for
880 HighResMIP, *Geosci. Model Dev.*, 11, 3681–3712, <https://doi.org/10.5194/gmd-11-3681-2018>,
881 2018b.

882

883 Roberts, M. J., Baker, A., Blockley, E. W., Calvert, D., Coward, A., Hewitt, H. T., Jackson, L. C.,
884 Kuhlbrodt, T., Mathiot, P., Roberts, C. D., Schiemann, R., Seddon, J., Vannière, B., and Vidale, P.
885 L.: Description of the resolution hierarchy of the global coupled HadGEM3-GC3.1 model as
886 used in CMIP6 HighResMIP experiments, *Geosci. Model Dev.*, [https://doi.org/10.5194/gmd-](https://doi.org/10.5194/gmd-12-4999-2019)
887 12-4999-2019, 2019.

888

889 Sørland, S. L., Schär, C., Lüthi, D. And Kjellström, E.: Bias patterns and climate change signals in
890 GCM-RCM model chains, *Environ. Res. Lett.*, 13, 074017, <https://doi.org/10.1088/1748-9326/aacc7>,
891 2018.

892

893 Stephens, G. L., L'Ecuyer, T., Forbes, R., Gettelmen, A., Golaz, J.-C., Bodas-Salcedo, A., Suzuki, K.,
894 Gabriel, P. and Haynes, J.: Dreary state of precipitation in global models. *J Geophys Res*, 115, D24211.
895 [doi:10.1029/2010JD014532](https://doi.org/10.1029/2010JD014532), 2010.

896

897 Stratton, R. A. and Stirling, A. J.: Improving the diurnal cycle of convection in GCMs, *Q. J. R. Meteorol.*
898 *Soc.*, 138, 1121–1134, [doi:10.1002/qj.991](https://doi.org/10.1002/qj.991), 2012.

899
900
901
902
903
904
905

906
907
908
909

910
911
912
913
914
915
916
917
918
919
920
921
922
923
924
925
926

Taylor, K. E., Stouffer, R. J., and Meehl, G. A.: An overview of CMIP5 and the experiment design, Bull. Amer. Meteor. Soc., 93, 485-498, DOI:10.1175/BAMS-D-11-00094.1, 2012.

van Haren, R., R. J. Haarsma, G. J. Van Oldenborgh, and W. Hazeleger, 2015: Resolution Dependence of European Precipitation in a State-of-the-Art Atmospheric General Circulation Model. J. Climate, 28, 5134–5149, <https://doi.org/10.1175/JCLI-D-14-00279.1>.

Vautard, R., Kadygrov, N., Iles, C., Boberg, F., Buonomo, E., Bülow, K., et al. 2020: Evaluation of the large EURO-CORDEX regional climate model ensemble. Journal of Geophysical Research: Atmospheres, 125, e2019JD032344. Accepted Author Manuscript. <https://doi.org/10.1029/2019JD032344>

Vergara-Temprado, J., Ban, N., Panosetti, D., Schlemmer, L., and Schär, C.: Climate models permit convection at much coarser resolutions than previously considered, J. Clim., JCLI-D-19-0286.1. doi:10.1175/JCLI-D-19- 0286.1, 2019.

Voltaire, A., Saint-Martin, D., Sénési, S., Decharme, B., Alias, A., Chevallier, M., Colin, J., Guérémy, J.-F., Michou, M., Moine, M.-P., Nabat, P., Roehrig, R., Salas y Méliá, D., Séférián, R., Valcke, S., Beau, I., Belamari, S., Berthet, S., Cassou, C., Cattiaux, J., Deshayes, J., Douville, H., Franchisteguy, L., Ethé, C., Geoffroy, O., Lévy, C., Madec, G., Meurdesoif, Y., Msadek, R., Ribes, A., Sanchez-Gomez, E., and Terray, L.: Evaluation of CMIP6 DECK Experiments with CNRM-CM6-1, J. Adv. Model. Earth Syst., 11, 2177–2213, <https://doi.org/10.1029/2019MS001683>, 2019.

Welch, B. L.: The generalization of ‘students’ problem when several different population variances are involved, Biometrika, Volume 34, Issue 1-2, January 1947, Pages 28–35, <https://doi.org/10.1093/biomet/34.1-2.28>, 1947.

927 Zappa, G., Shaffrey, L. C., and Hodges, K. I.: The Ability of CMIP5 Models to Simulate North Atlantic
928 Extratropical Cyclones, *J. Climate*, 26, 5379–5396, <https://doi.org/10.1175/JCLI-D-12-00501.1>, 2013.
929
930

932 **Tables**

| Ensemble | Model | Contact institute | Atmo- spheric grid spacing |
|-----------------|---------------|--------------------------------------------------------------------------------------------------------------------------------------------------------------------------------------------------------------|-----------------------------------------------|
| CMIP5 | ACCESS1-0 | Commonwealth Scientific and Industrial Research Organisation, Australia, and Bureau of Meteorology | N96 |
| CMIP5 | ACCESS1-3 | Commonwealth Scientific and Industrial Research Organisation, Australia, and Bureau of Meteorology | N96 |
| CMIP5 | CanESM2 | Canadian Centre for Climate Modelling and Analysis | T63 |
| CMIP5 | CMCC-CESM | Centro Euro-Mediterraneo per i Cambiamenti Climatici | 96x48 |
| CMIP5 | CMCC-CM | Centro Euro-Mediterraneo per i Cambiamenti Climatici | 480x240 |
| CMIP5 | CMCC-CMS | Centro Euro-Mediterraneo per i Cambiamenti Climatici | 192x96 |
| CMIP5 | CSIRO-Mk3-6-0 | Australian Commonwealth Scientific and Industrial Research Organization (CSIRO) Marine and Atmospheric Research in collaboration with the Queensland Climate Change Centre of Excellence (QCCCE) | T63 |
| CMIP5 | FGOALS-g2 | Institute of Atmospheric Physics, Chinese Academy of Sciences and Tsinghua University | 128x60 |
| CMIP5 | GFDL-CM3 | NOAA Geophysical Fluid Dynamics Laboratory | 144x90 |
| CMIP5 | GFDL-ESM2G | NOAA Geophysical Fluid Dynamics Laboratory | 144x90 |
| CMIP5 | HadCM3 | Met Office Hadley Centre | 96x73 |
| CMIP5 | HadGEM2-CC | Met Office Hadley Centre | N96 |
| CMIP5 | HadGEM2-ES | Met Office Hadley Centre | N96 |
| CMIP5 | IPSL-CM5A-LR | Institut Pierre Simon Laplace | 96x96 |
| CMIP5 | IPSL-CM5A-MR | Institut Pierre Simon Laplace | 144x143 |

| | | | |
|-----------|-----------------|--------------------------------------------------------------------------------------------------------------------------------------------------------------------------------------------------------------|---------|
| CMIP5 | MPI-ESM-LR | Max Planck Institute for Meteorology | T63 |
| CMIP5 | MPI-ESM-MR | Max Planck Institute for Meteorology | T63 |
| CMIP5 | NorESM1-M | Norwegian Climate Centre | 144x96 |
| CMIP6 | ACCESS-CM2 | Commonwealth Scientific and Industrial Research Organisation, Australia, and Bureau of Meteorology | 192x145 |
| CMIP6 | ACCESS-ESM1-5 | Commonwealth Scientific and Industrial Research Organisation, Australia, and Bureau of Meteorology | 192x145 |
| CMIP6 | CESM2-FV2 | The National Center for Atmospheric Research | 144x96 |
| CMIP6 | CESM2 | The National Center for Atmospheric Research | 288x192 |
| CMIP6 | CESM2-WACCM-FV2 | The National Center for Atmospheric Research | 144x96 |
| CMIP6 | CESM2-WACCM | The National Center for Atmospheric Research | 288x192 |
| CMIP6 | EC-Earth3 | EC-Earth-Consortium | 512x256 |
| CMIP6 | EC-Earth3-Veg | EC-Earth-Consortium | 512x256 |
| CMIP6 | GFDL-CM4 | NOAA Geophysical Fluid Dynamics Laboratory | 360x180 |
| CMIP6 | INM-CM4-8 | Institute for Numerical Mathematics, Russian Academy of Science | 180x120 |
| CMIP6 | INM-CM5-0 | Institute for Numerical Mathematics, Russian Academy of Science | 180x120 |
| CMIP6 | MIROC6 | Japan Agency for Marine-Earth Science and Technology, Atmosphere and Ocean Research Institute, The University of Tokyo, National Institute for Environmental Studies, RIKEN Center for Computational Science | T85 |
| CMIP6 | MPI-ESM-1-2-HAM | Max Planck Institute for Meteorology | 192x96 |
| CMIP6 | MPI-ESM1-2-LR | Max Planck Institute for Meteorology | 192x96 |
| CMIP6 | MRI-ESM2-0 | Meteorological Research Institute, Tsukuba | 320x160 |
| CMIP6 | NorCPM1 | Norwegian Climate Centre | 320x384 |
| CMIP6 | NorESM2-LM | Norwegian Climate Centre | 144x96 |
| CMIP6 | NorESM2-MM | Norwegian Climate Centre | 288x192 |
| CMIP6 | SAM0-UNICON | Seoul National University | 288x192 |
| PRIMAVERA | CNRM-CM6-1 | CNRM-CERFACS | 256x128 |
| PRIMAVERA | CNRM-CM6-1-HR | CNRM-CERFACS | 720x360 |
| PRIMAVERA | EC-Earth3 | EC-Earth-Consortium | 512x256 |

| | | | |
|-----------|-----------------|-------------------------------------------------------|----------|
| PRIMAVERA | EC-Earth3-HR | EC-Earth-Consortium | 1024x512 |
| PRIMAVERA | IFS-HR | European Centre for Medium-Range Weather Forecasts | 720x360 |
| PRIMAVERA | IFS-LR | European Centre for Medium-Range Weather Forecasts | 360x180 |
| PRIMAVERA | HadGEM3-GC31-HM | Met Office Hadley Centre | 1024x720 |
| PRIMAVERA | HadGEM3-GC31-LM | Met Office Hadley Centre | 192x144 |
| PRIMAVERA | HadGEM3-GC31-MM | Met Office Hadley Centre | 432x324 |
| PRIMAVERA | MPIESM-1-2-HR | Max Planck Institute for Meteorology | 384x192 |
| PRIMAVERA | MPIESM-1-2-XR | Max Planck Institute for Meteorology | 768x384 |

Table 1. The GCM ensembles used in this study and the GCMs they consist of. Grid spacing is given in the same format as in the meta data for each model.

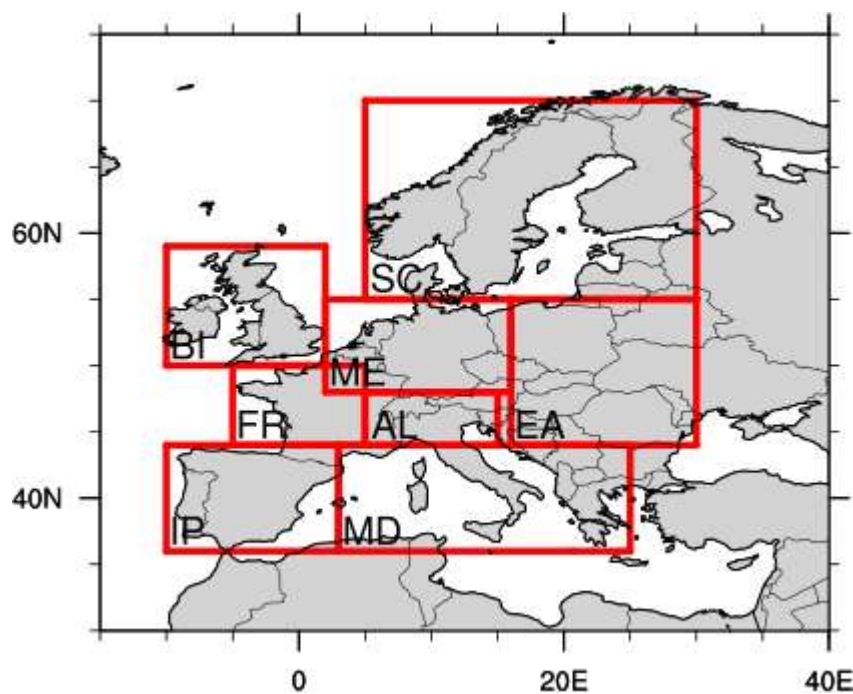
| Institute | RCM | Driving GCM | | | | | | | | | |
|-----------|------------|-------------|---|---|----|---|----|----|---|----|----|
| | | 1 | 2 | 3 | 4 | 5 | 6 | 7 | 8 | 9 | 10 |
| CLMcom | CCLM4-8-17 | x | x | | x | | x | | x | xo | |
| CNRM | ALADIN53 | | x | | | | | | | | |
| CNRM | ALADIN63 | | x | | | | | | | | |
| DMI | HIRHAM5 | | | | xo | | x | | | | x |
| GERICS | REMO2015 | x | x | | x | | x | | x | | x |
| IPSL | WRF331F | | | | | | | xo | | | |
| KNMI | RACMO22E | | | | xo | | o | | | | x |
| MPI-CSC | REMO2009 | | | | | | | | | xo | |
| SMHI | RCA4 | o | o | o | xo | o | xo | xo | o | xo | o |
| UHOH | WRF361H | | | | | | x | | | x | |
| HMS | ALADIN52 | | o | | | | | | | | |

Table 2. RCM GCM combinations used in this study. EURO-CORDEX simulations at 0.11° (~12.5 km) are marked with “x” and at 0.44° (~50 km) are marked with “o”. The driving GCMs are: 1) CanESM2, 2) CNRM-CM5, 3) CSIRO-Mk3-6-0, 4) EC-Earth, 5) GFDL-ESM2M, 6) HadGEM2-ES, 7) IPSL-CM5A-MR, 8) MIROC5, 9) MPI-ESM-LR, 10) NorESM1-M

| Short | Long name | Definition | Unit |
|-------|-----------|------------|------|
|-------|-----------|------------|------|

| name | | | |
|--------|--------------------------------------|---------------------------------------------------------------------------------|-------------------------|
| RR1 | Wet days index | Number of days with precipitation sum equal to or more than 1 mm | Days year ⁻¹ |
| R20mm | Very heavy precipitation days index | Number of days with precipitation more than 20 mm | Days year ⁻¹ |
| SDII | Simple daily intensity index | Average precipitation sum on days with precipitation sum equal to or above 1 mm | mm day ⁻¹ |
| Rx1day | Highest one day precipitation amount | Precipitation amount on the day with highest amount | mm day ⁻¹ |

Table 3. Definitions of indices



945
 946 **Figure 1: The regions for which precipitation data is analysed: Scandinavia (SC), British Isles (BI), Mid-Europe (ME), France**
 947 **(FR), The Alps (AL), Eastern Europe (EA), Iberian Peninsula (IP) and the Mediterranean (MD).**

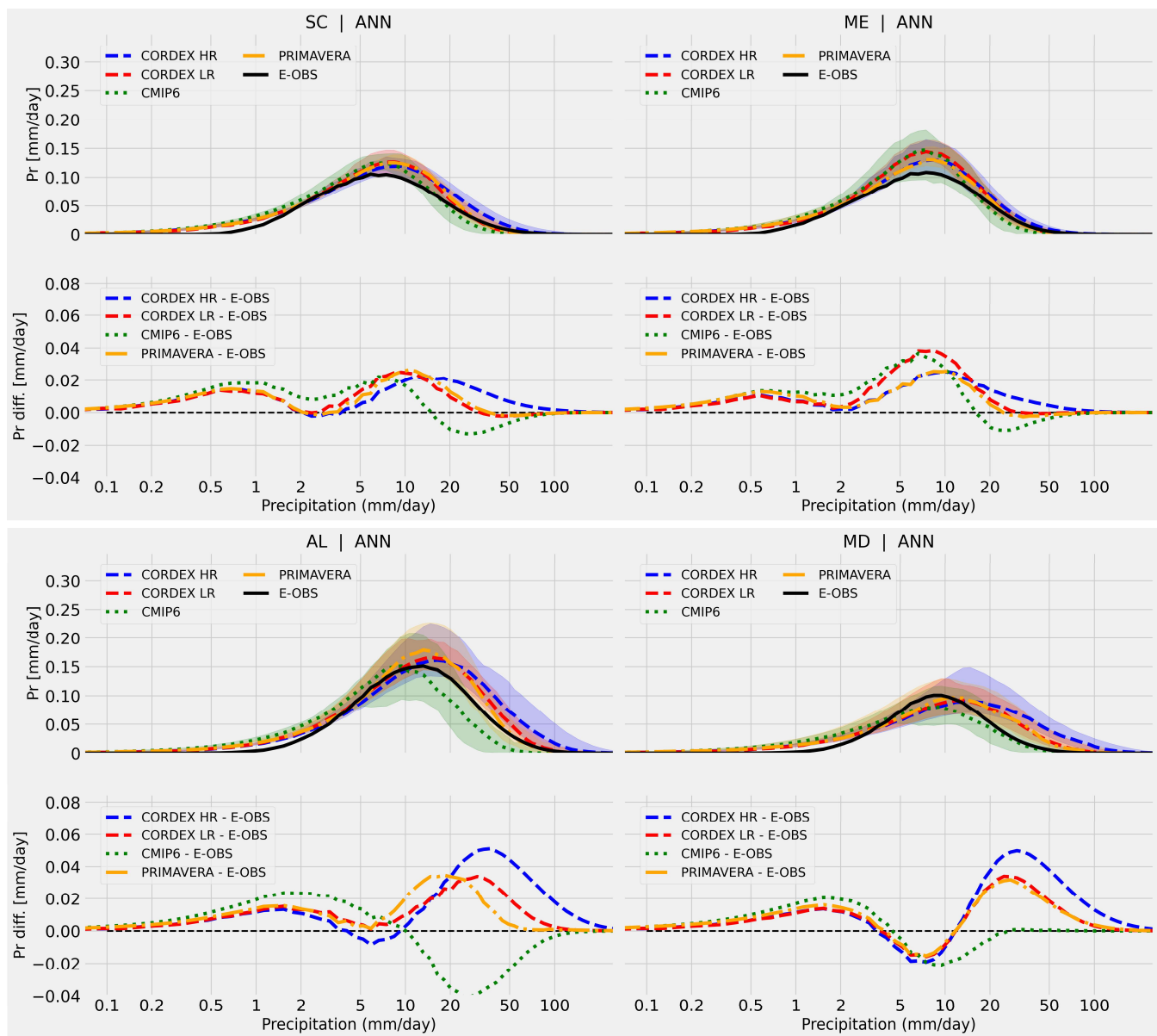


Figure 2: The panels show the actual contribution (to the total median precipitation, y-axis) per precipitation intensity bin (x-axis), based on annual (ANN) daily precipitation values in the CMIP6 (green dotted lines and shading), PRIMAVERA (orange dashed-dotted lines and shading), CORDEX low resolution (red dashed lines and shading) and CORDEX high resolution (blue dashed lines and shading) ensembles. The displayed regions are Scandinavia (SC, top left), mid-Europe (ME, top right), the Alps (AL, bottom left) and the Mediterranean (MD, bottom right). Coloured shadings represent the 5-95 percentile range in respective ensemble. Black solid lines are E-OBS (0.1° resolution) observations.

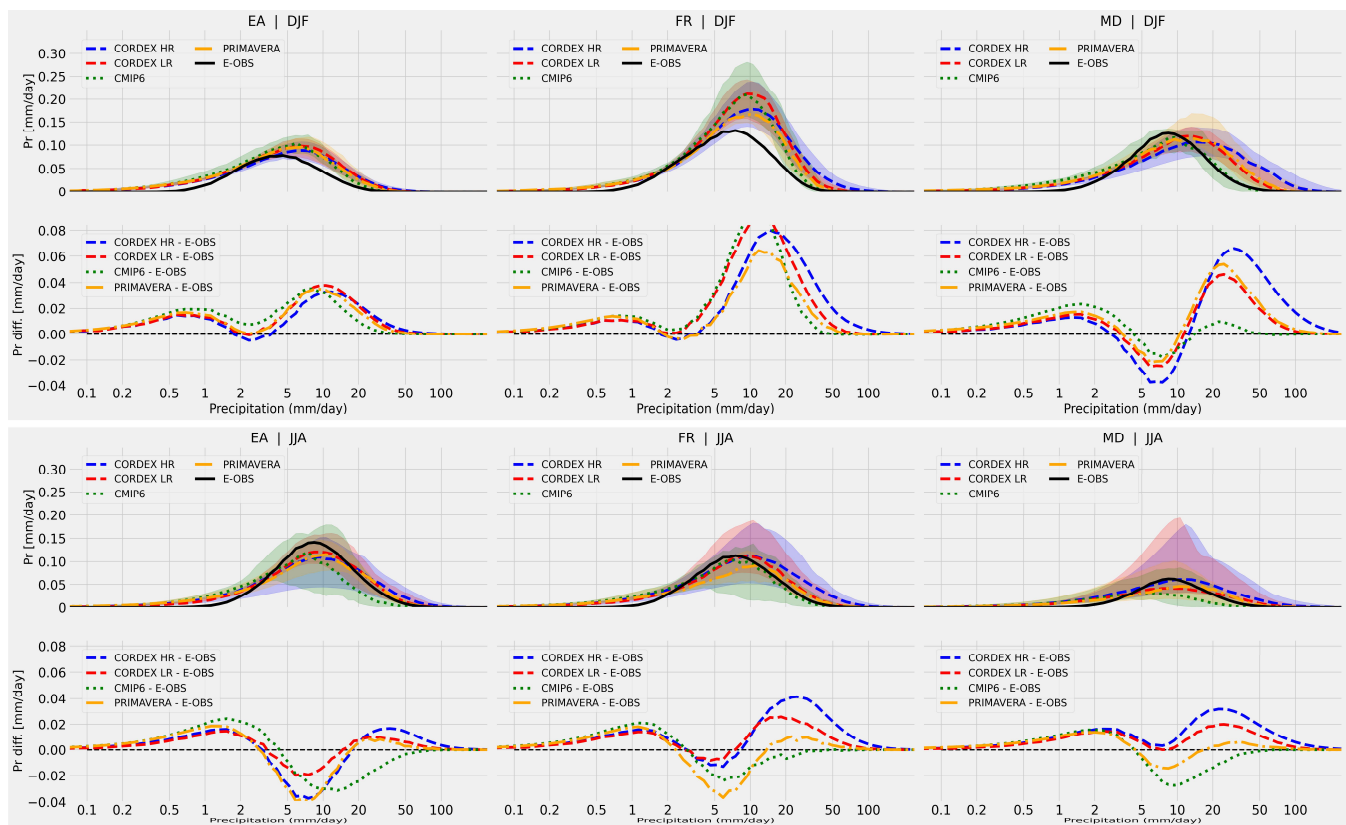


Figure 3: Same as in Fig. 2 but for DJF (top row) and JJA (bottom row) daily precipitation values and for the eastern Europe (EA, left), France (FR, middle) and the Mediterranean (MD, right) regions. Coloured shadings represent the 5-95 percentile range in respective ensemble. Black solid lines are E-OBS (0.1° resolution) observations.

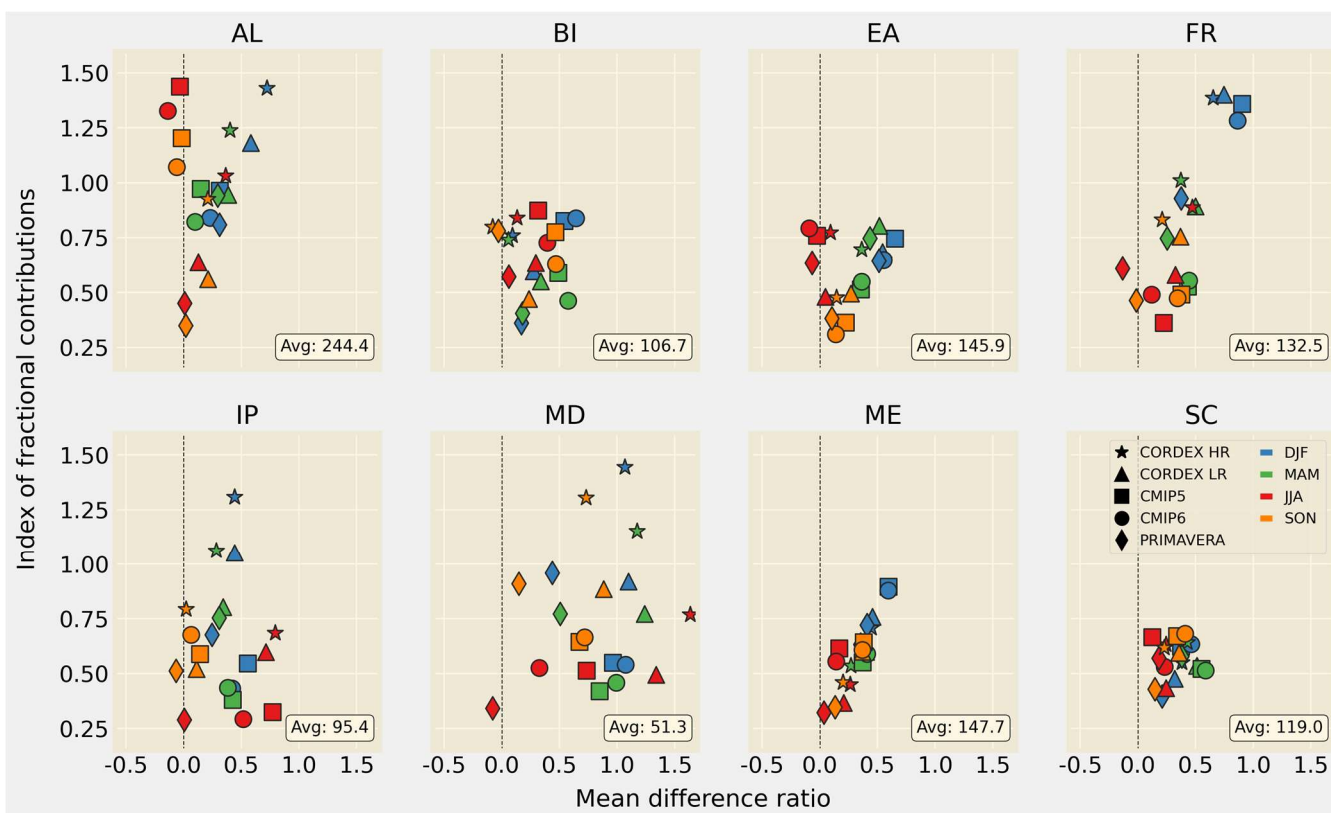


Figure 4: The index of fractional contributions (y-axis) plotted as a function of the fractional difference in seasonal total precipitation (x-axis). E-OBS (0.1° resolution) is the reference data set and E-OBS average annual total precipitation (in mm year⁻¹) is shown in lower right in each panel.

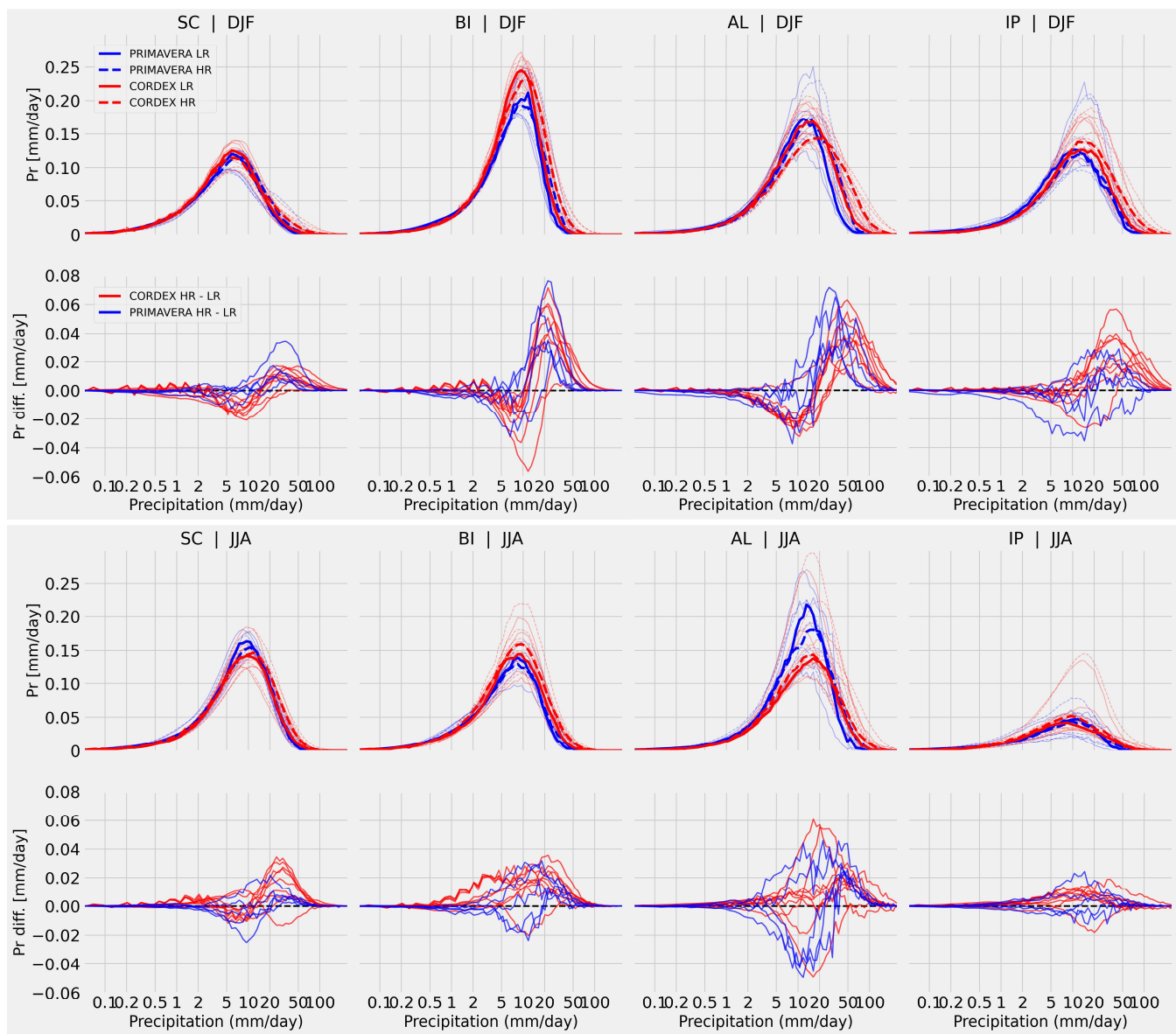


Figure 5: The panels show the actual contribution (to the total mean precipitation, y-axis) per precipitation intensity bin (x-axis), based on DJF (top row) and JJA (bottom row) daily mean precipitation values in CORDEX and PRIMAVERA models for the Scandinavia (SC), British Isles (BI), the Alps (AL) and Iberian Peninsula (IP) regions. Thin lines in upper part of each panel represent each individual model while the thick lines represent the ensemble means. In the lower part of each panel each line represents differences between respective high- and low-resolution model pair.

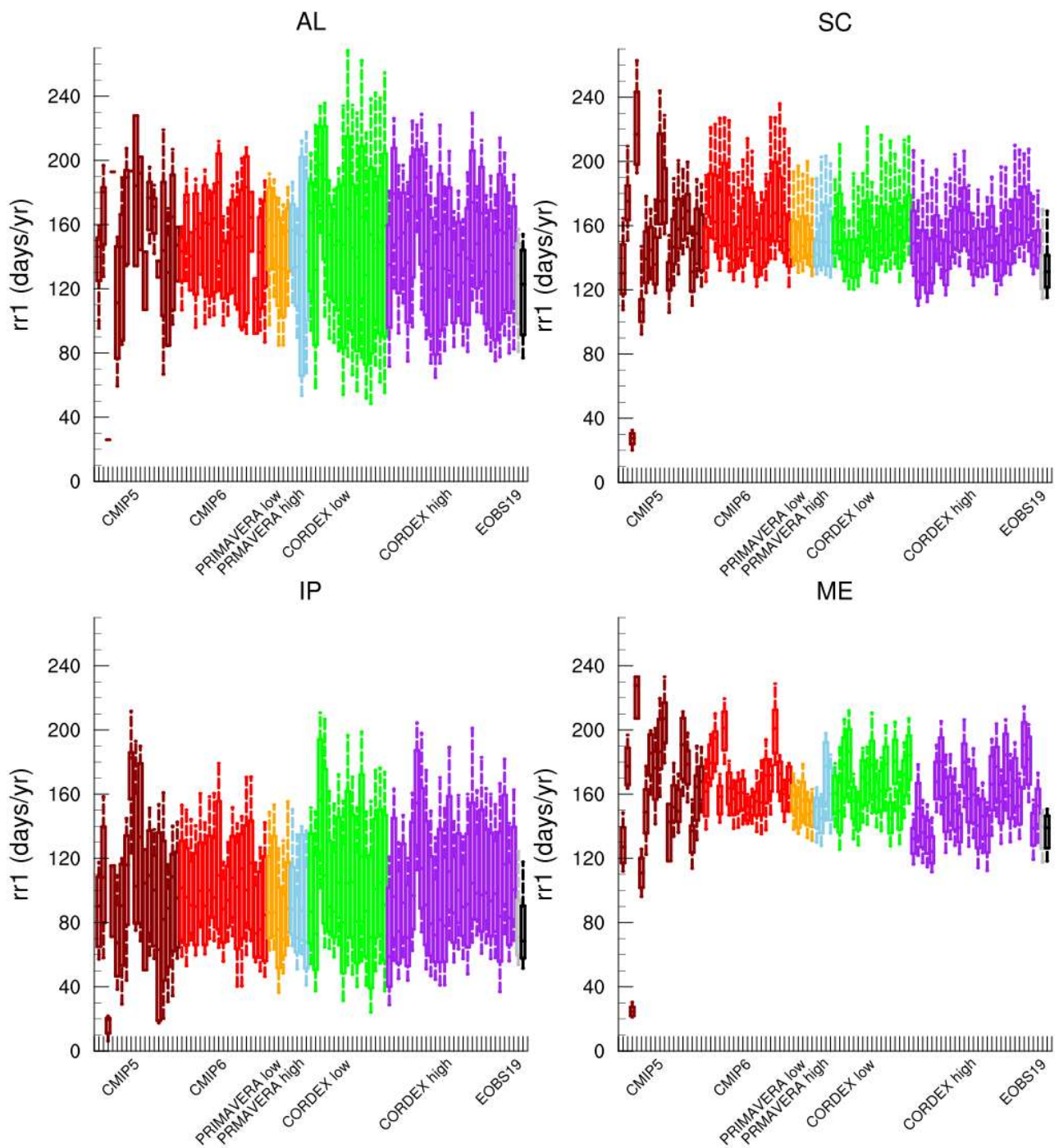
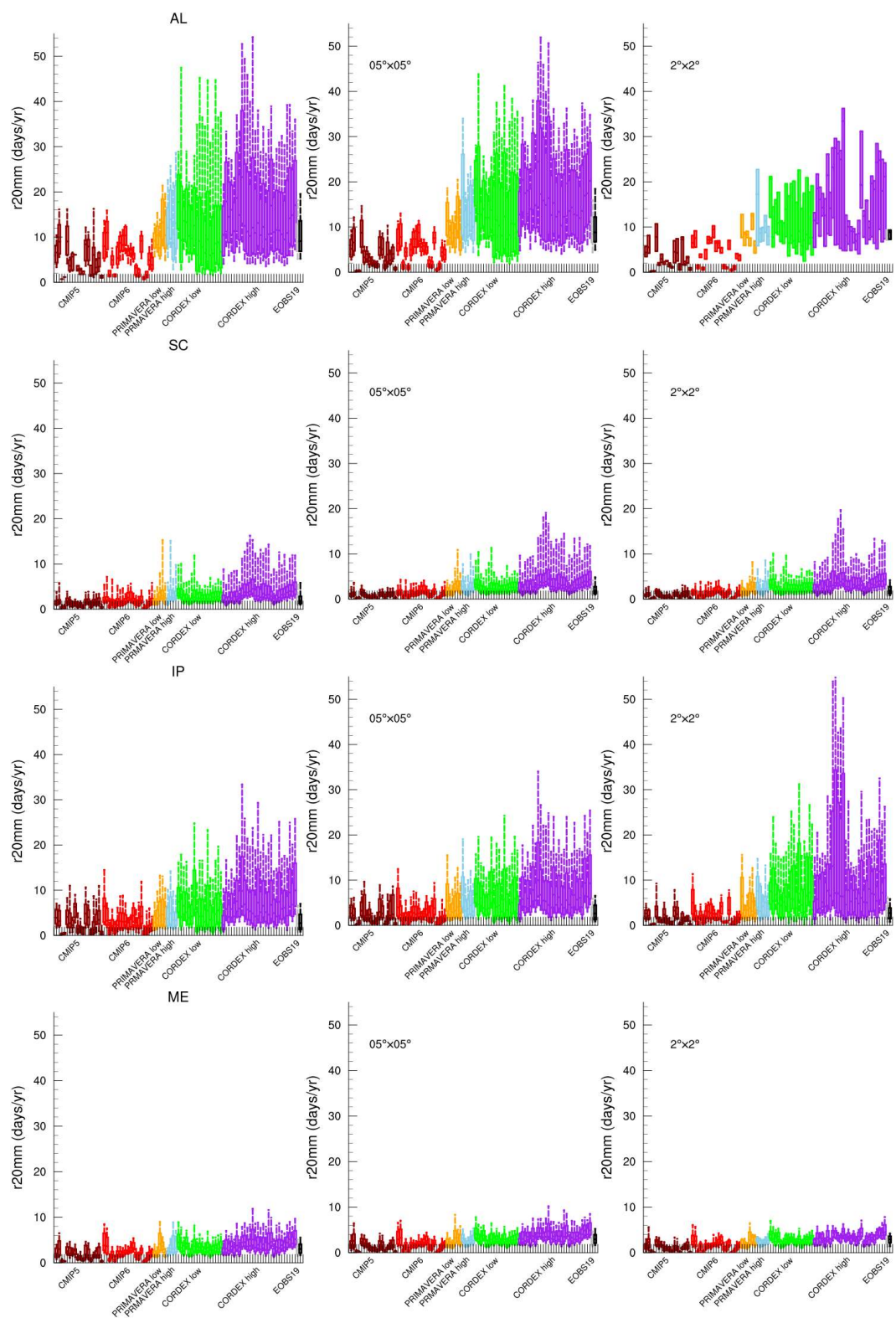
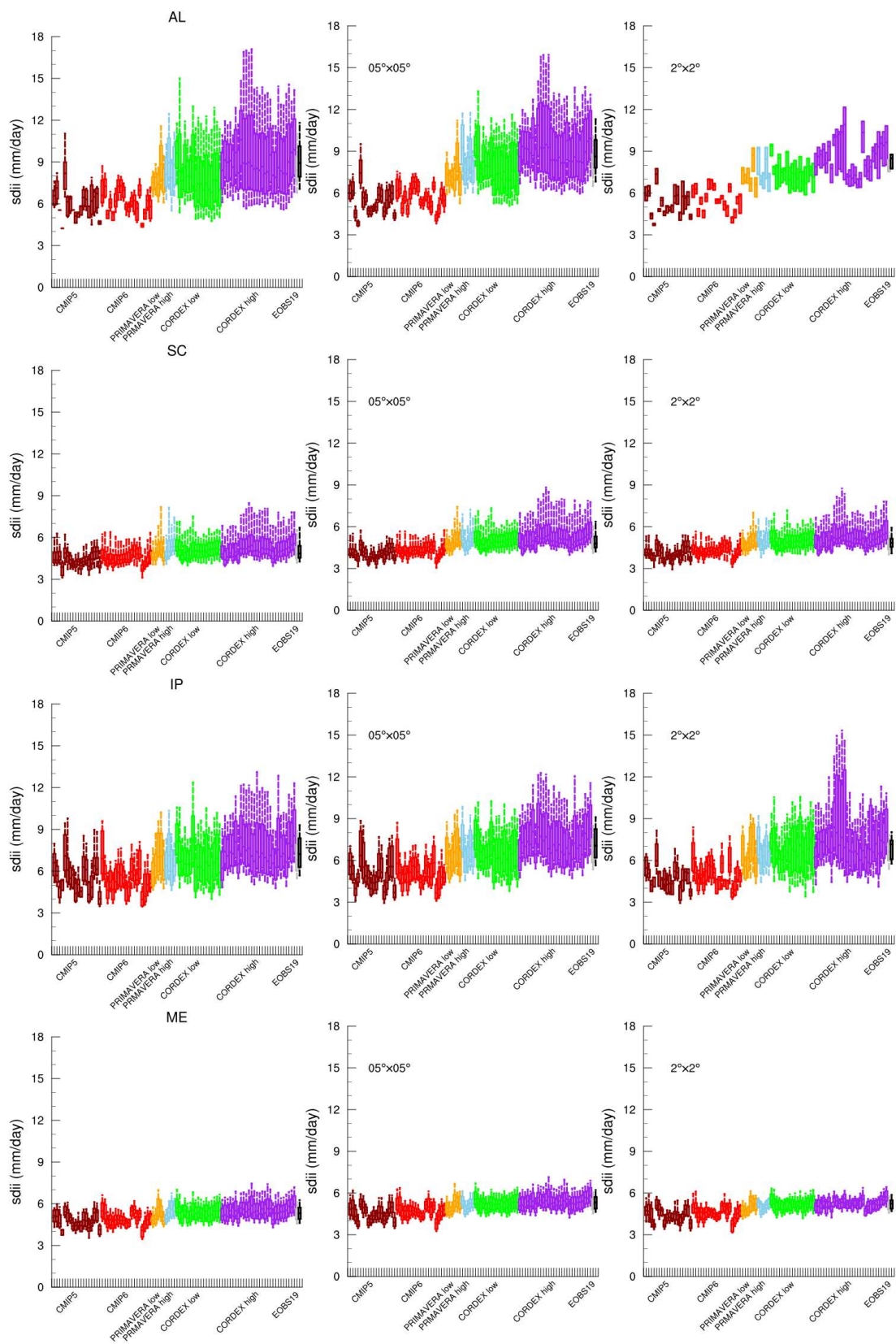


Figure 6. Number of precipitation days (RR1 (days year⁻¹)) in the Alps (AL, top left), Scandinavia (SC, top right), the Iberian Peninsula (IP, bottom left) and mid-Europe (ME, bottom right) for individual models in the CMIP5 (brown), CMIP6 (red), PRIMAVERA LR (orange), PRIMAVERA HR (light blue), CORDEX LR (green) and CORDEX HR (purple) ensembles as well as E-OBS at 28 (grey) and 11 km (black). Boxes mark the 25th and 75th percentile, with the median inside; whiskers go from the 10th to the 90th percentile.



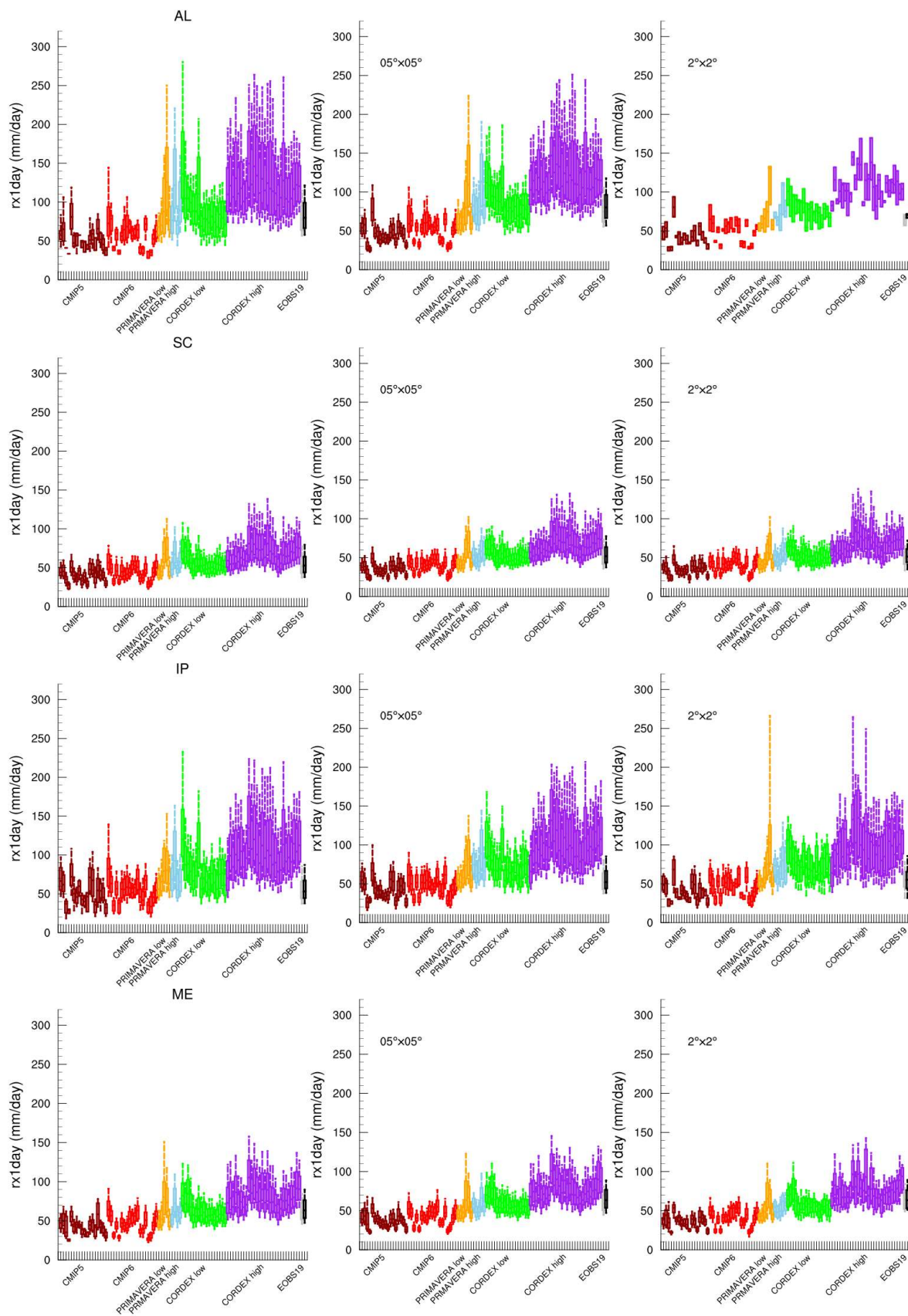
976 Figure 7. Same as Figure 6 but for the number of days with precipitation amount over 20 mm (R20mm (days year⁻¹)). Left column:
977 model data on their original grids, centre column: all data regridded to 0.5°×0.5° grid, right column: all data regridded to 2°×2°
978 grid.

979



981 **Figure 8. Same as Figure 7 but for the simple precipitation intensity index (SDII (mm day⁻¹)).**

982



984 **Figure 9. Same as Figure 7 but for the maximum one day precipitation (Rx1day (mm day⁻¹)).**

985

986

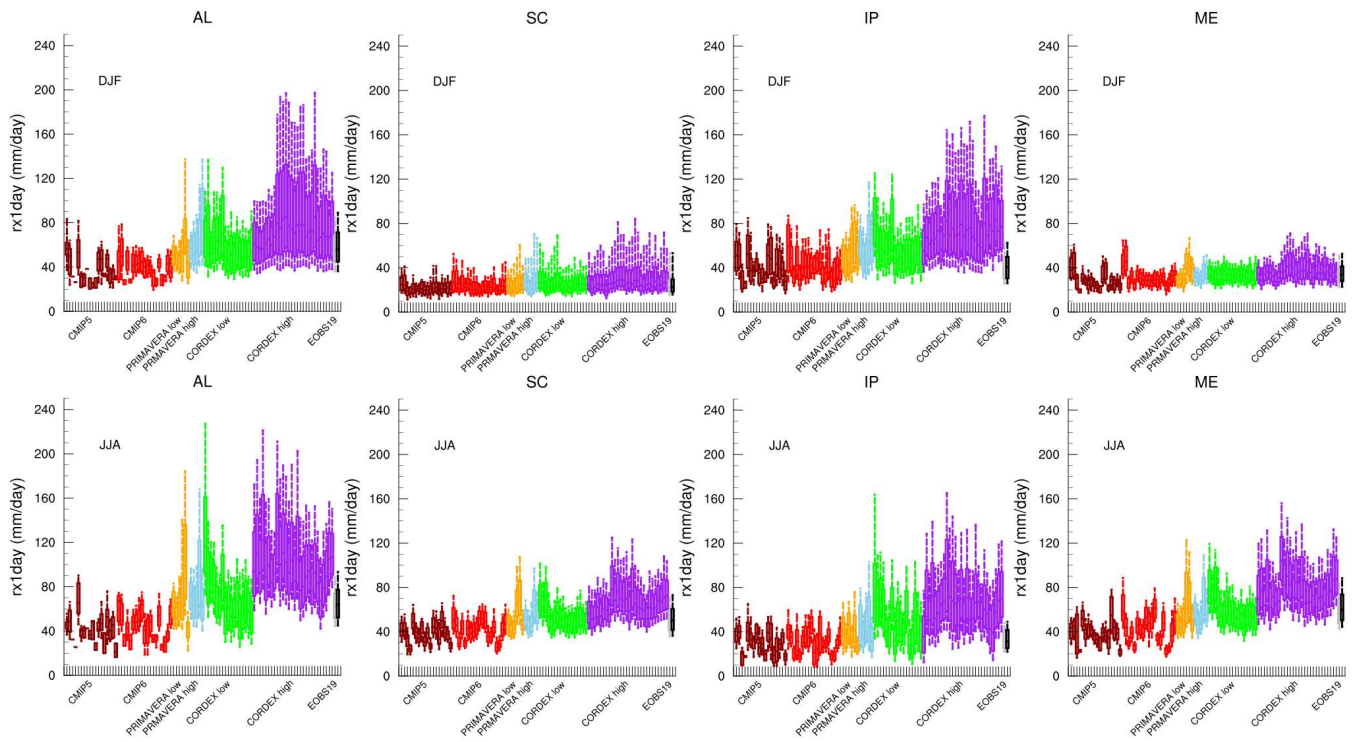


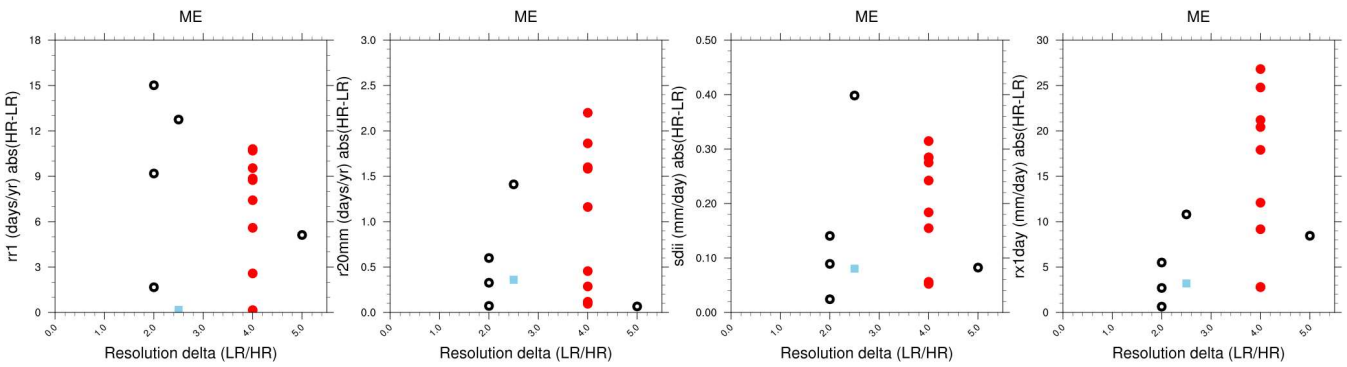
Figure 10. Same as Figure 6 but for the maximum one-day precipitation ($Rx1day$ ($mm\ day^{-1}$)), top row: winter (DJF), bottom row: summer (JJA).



991 Figure 11. Number of precipitation days (RR1 (days year⁻¹), first row), number of days with precipitation amount over 20 mm
992 (R20mm (days year⁻¹), second row), simple precipitation intensity index (SDII (mm day⁻¹), third row), maximum one day
993 precipitation (Rx1day (mm day⁻¹), fourth row) in the Mid-European region (ME) in the PRIMAVERA LR (pink) and HR (red)
994 models, CORDEX LR (light blue) and HR (purple) models as well as E-OBS LR (grey) and HR (black). Left column: model data
995 on their original grids, centre column: all data regridded to 0.5°×0.5° grid, right column: all data regridded to 2°×2° grid. Boxes
996 mark the 25th and 75th percentile, with the median inside; whiskers go from the 10th to the 90th percentile. If the the high-resolution
997 version of a model is significantly different from the low-resolution version this is marked with a vertical line in the high-resolution
998 boxes.

999

1000



1001

1002

1003

1004

1005

1006

Figure 12. Absolute difference between HR and LR version of PRIMAVERA (black rings), CORDEX (red circles) and E-OBS (blue squares) in precipitation days (RR1 (days year⁻¹), first column, number of days with precipitation amount over 20 mm (R20mm (days year⁻¹), second column), simple precipitation intensity index (SDII (mm day⁻¹), third column), maximum one day precipitation (Rx1day (mm day⁻¹), fourth column) in the Mid-European region (ME). X-axes show the resolution delta (LR/HR) for each model (example: 50 km grid spacing divided by 12.5 km equals 4).